


RESEARCH ARTICLE

C-Terminal Tyrosine Residue Modifications Modulate the Protective Phosphorylation of Serine 129 of α -Synuclein in a Yeast Model of Parkinson's Disease

Alexandra Kleinknecht^{1,2}, Blagovesta Popova^{1,2}, Diana F. Lázaro^{2,3}, Raquel Pinho^{2,3,4}, Oliver Valerius¹, Tiago F. Outeiro^{2,3,5}, Gerhard H. Braus^{1,2*}

1 Department of Molecular Microbiology and Genetics and Göttingen Center for Molecular Biosciences (GZMB), Institute of Microbiology and Genetics, Georg-August-Universität, Göttingen, Germany, **2** Center for Nanoscale Microscopy and Molecular Physiology of the Brain (CNMPB), Göttingen, Germany, **3** Department of NeuroDegeneration and Restorative Research, University of Göttingen Medical School, Göttingen, Germany, **4** Faculty of Medicine, University of Porto, Porto, Portugal, **5** Max Planck Institute for Experimental Medicine, Göttingen, Germany

 These authors contributed equally to this work.

* gbraus@gwdg.de



CrossMark
click for updates

 OPEN ACCESS

Citation: Kleinknecht A, Popova B, Lázaro DF, Pinho R, Valerius O, Outeiro TF, et al. (2016) C-Terminal Tyrosine Residue Modifications Modulate the Protective Phosphorylation of Serine 129 of α -Synuclein in a Yeast Model of Parkinson's Disease. *PLoS Genet* 12(6): e1006098. doi:10.1371/journal.pgen.1006098

Editor: Bingwei Lu, Stanford University School of Medicine, UNITED STATES

Received: December 22, 2015

Accepted: May 10, 2016

Published: June 24, 2016

Copyright: © 2016 Kleinknecht et al. This is an open access article distributed under the terms of the [Creative Commons Attribution License](https://creativecommons.org/licenses/by/4.0/), which permits unrestricted use, distribution, and reproduction in any medium, provided the original author and source are credited.

Data Availability Statement: All relevant data are within the paper.

Funding: This work was funded by the DFG Cluster of Excellence and DFG Research Center Nanoscale Microscopy and Molecular Physiology of the Brain (CNMPB). RP is supported by a PhD fellowship from FCT Portugal (SFRH/BD/80884/2011). The funders had no role in study design, data collection and analysis, decision to publish, or preparation of the manuscript.

Abstract

Parkinson's disease (PD) is characterized by the presence of proteinaceous inclusions called Lewy bodies that are mainly composed of α -synuclein (α Syn). Elevated levels of oxidative or nitrative stresses have been implicated in α Syn related toxicity. Phosphorylation of α Syn on serine 129 (S129) modulates autophagic clearance of inclusions and is prominently found in Lewy bodies. The neighboring tyrosine residues Y125, Y133 and Y136 are phosphorylation and nitration sites. Using a yeast model of PD, we found that Y133 is required for protective S129 phosphorylation and for S129-independent proteasome clearance. α Syn can be nitrated and form stable covalent dimers originating from covalent cross-linking of two tyrosine residues. Nitrated tyrosine residues, but not di-tyrosine-crosslinked dimers, contributed to α Syn cytotoxicity and aggregation. Analysis of tyrosine residues involved in nitration and crosslinking revealed that the C-terminus, rather than the N-terminus of α Syn, is modified by nitration and di-tyrosine formation. The nitration level of wild-type α Syn was higher compared to that of A30P mutant that is non-toxic in yeast. A30P formed more dimers than wild-type α Syn, suggesting that dimer formation represents a cellular detoxification pathway in yeast. Deletion of the yeast flavohemoglobin gene *YHB1* resulted in an increase of cellular nitrative stress and cytotoxicity leading to enhanced aggregation of A30P α Syn. *Yhb1* protected yeast from A30P-induced mitochondrial fragmentation and peroxynitrite-induced nitrative stress. Strikingly, overexpression of neuroglobin, the human homolog of *YHB1*, protected against α Syn inclusion formation in mammalian cells. In total, our data suggest that C-terminal Y133 plays a major role in α Syn aggregate clearance by supporting the protective S129 phosphorylation for autophagy and by promoting proteasome clearance. C-terminal tyrosine nitration increases pathogenicity and can only be partially detoxified by α Syn di-tyrosine dimers. Our findings uncover a

Competing Interests: The authors have declared that no competing interests exist.

complex interplay between S129 phosphorylation and C-terminal tyrosine modifications of α Syn that likely participates in PD pathology.

Author Summary

Parkinson's disease is characterized by loss of dopaminergic neurons in midbrain and the presence of α Syn protein inclusions. Human α Syn mimics the disease pathology in yeast resulting in cytotoxicity and aggregate formation. α Syn is abundantly phosphorylated at serine S129 and possesses four tyrosines (Y39, Y125, Y133, and Y136) that can be post-translationally modified by nitration or phosphorylation. The consequence of each of these possible modifications is still unclear. Nitration as consequence of oxidative stress is a hallmark for neurodegenerative diseases. Here, we addressed the molecular mechanism, how tyrosine posttranslational modifications affect α Syn cytotoxicity. Tyrosine nitration can contribute to α Syn toxicity or can be part of a cellular salvage pathway when di-tyrosine-crosslinked dimers are formed. The Y133 residue, which can be either phosphorylated or nitrated, determines whether S129 is protectively phosphorylated and α Syn inclusions are cleared. This interplay with S129 phosphorylation demonstrates a dual role for C-terminal tyrosine residues. Yeast flavohemoglobin Yhb1 and its human counterpart neuroglobin NGB protect cells against cytotoxicity and aggregate formation. These novel insights into the molecular pathways responsible for α Syn cytotoxicity indicate NGB as a potential target for therapeutic intervention in PD.

Introduction

Parkinson's disease (PD) is one of the most common neurodegenerative diseases and affects about 1% of the population older than 60 years [1]. PD proceeds with selective loss of dopamine-producing neurons of the *substantia nigra pars compacta* in the ventral midbrain [2, 3]. Degeneration also occurs in other neuron types. Particularly, the mid-section of the *substantia nigra (zona compacta)* is affected by neurodegeneration, which is accompanied by the loss of neuromelanin pigment neurons leading to depigmentation [4, 5]. Loss of nigral dopaminergic neurons consequently results in dopamine depletion in the striatum and generates a wide range of motoric malfunctions [6]. PD is also described to be associated with non-motoric and non-dopaminergic symptoms that extend beyond the nigrostriatal dopamine pathway and often occur years or even decades prior to the clinical diagnosis [7, 8]. Typical hallmark of PD is the formation of Lewy bodies that can be observed in *post mortem* brain histology. Lewy bodies are intracellular proteinaceous inclusions with α -synuclein (α Syn) as major constituent [9–11]. Several independent point mutations in the α Syn encoding gene, as well as duplications or triplications of the wild-type α Syn locus, have been found in rare familial inherited forms of PD [12–18]. This makes α Syn a hallmark protein for PD and other related diseases, which are summarized as synucleinopathies. α Syn is a natively unfolded protein, enriched at presynaptic nerve terminals. The nuclear localization of α Syn remains under debate, since conflicting results have been obtained for the existence of α Syn in nuclei of mammalian brain neurons [19–23]. α Syn was also reported to be localized in the nucleus of cultured neurons, where it may impair histone acetylation and thereby promote neurotoxicity [24, 25]. α Syn is involved in the modulation of synaptic activity through regulation of SNARE-complex assembly of

presynaptic vesicles, regulation of neurotransmitter release, regulation of cell differentiation and phospholipid metabolism [26–31].

Posttranslational modifications (PTMs) play an important role in regulating α Syn aggregation propensity and cytotoxicity. Major PTMs of α Syn include phosphorylation, ubiquitination, sumoylation or nitration [32–36]. The predominant α Syn modification is phosphorylation at serine 129 (S129). More than 90% of α Syn in Lewy bodies is phosphorylated at this residue, whereas only 4% of the soluble protein is accordingly modified [37]. The molecular function of phosphorylation at S129 is still under debate [38]. This modification modulates clearance of α Syn inclusions in a yeast model of PD [39, 40]. In addition, phosphorylation at S129 can suppress the defects induced by impaired sumoylation such as increased number of cells with inclusions and reduced yeast growth [41]. These findings support a protective function for S129 phosphorylation in this model.

Nitrated α Syn represents another PTM discovered in Lewy bodies [33, 34]. Nitration might be involved in α Syn aggregation, thereby modulating α Syn-induced cytotoxicity. Oxidative and nitrative stresses are implicated in the pathogenesis of PD [33, 34, 42–45]. Neuroinflammation followed by nitration of α Syn causes accumulation of α Syn aggregates and neurodegeneration in mice [46]. Moreover, nitrated α Syn was observed to induce adaptive immune responses that exacerbate PD pathology in the MPTP mouse model [47]. Increased nitrated α Syn is present in peripheral blood mononuclear cells of idiopathic PD patients compared to healthy individuals [48]. These studies provide evidence for a direct link between nitrative damage and the onset and progression of neurodegenerative synucleinopathies. However, the precise molecular mechanism that leads to the formation of pathological inclusions is still elusive.

Exposure of α Syn to nitrative agents results in the formation of α Syn oligomers and higher molecular weight α Syn species that are resistant to strong denaturing conditions, suggesting that α Syn proteins are covalently crosslinked [42, 49–52]. This oligomerization can be abolished *in vitro* when α Syn lacks the four tyrosine residues at positions 39, 125, 133 and 136 [53]. Three of these four tyrosine residues are located at the C-terminal end of α Syn in close neighborhood to the protective S129 phosphorylation site. Nitrating agents such as peroxynitrite/ CO_2 (PON) can nitrate tyrosine to generate 3-nitrotyrosine. Alternatively, highly stable *o,o'*-di-tyrosine oligomers can be formed, including dimers, trimers and higher oligomeric species [42, 54–56]. However, the majority of the studies were performed *in vitro* after exposure of α Syn to nitrating agents leading to non-specific nitration at all tyrosine residues. It is still unclear, whether the nitration-modified α Syn intermediates are toxic and what are the functional consequences of these modifications. Even the precise positions or preferred combinations for the tyrosines involved in di-tyrosine formation *in vivo* are yet unknown.

The yeast *Saccharomyces cerevisiae* is an established eukaryotic model system used to uncover the correlation between structural features of α Syn and its toxicity. It provides a unique tool to study the molecular basis of PD *in vivo* [57, 58]. 44% of the yeast genes reveal significant sequence similarities that suggest homology to human genes [59]. The basic molecular machinery necessary for neuronal function is conserved between yeast and humans. Strikingly, heterologous expression of different forms of human α Syn in yeast cells recapitulates central features of PD, including dose-dependent toxicity and aggregation. Expression of wild-type α Syn, E46K and A53T mutant results in significant growth inhibition and formation of inclusions [60, 61]. An unusual feature of the yeast system, which is different from PD and other models, is that the A30P variant only forms inclusions when highly expressed and fails to display a growth inhibition in yeast, because aggregation of A30P is only transient [62, 63]. Aggregation of α Syn in yeast cells causes mitochondrial dysfunction or formation of

chemically reactive molecules, such as reactive oxygen species (ROS) and reactive nitrogen species (RNS), which is similar to mammalian cells [60, 64–69].

In this study, we analyzed the effects of nitration of wild-type and A30P mutant α Syn in yeast cells. We observed that the C-terminus of α Syn is preferentially modified by nitration compared to the N-terminus in soluble monomers as well as in dimers. Nitro- and phosphate-groups were found at Y133. Tyrosine nitration leads to increased aggregation and cytotoxicity of α Syn in yeast and confers toxicity to the non-toxic A30P mutant. The yeast nitric oxide oxidoreductase Yhb1 as well as human neuroglobin, which are encoded by homologous genes conserved from yeast to man, reduced the number of cells with inclusions and protected yeast from A30P-induced mitochondrial damage. One target of these enzymes is the C-terminal Y133 and we could show that it is required for protective phosphorylation of α Syn at S129. Our data revealed a complex choreography of posttranslational events at the α Syn C-terminus and suggest that tyrosine modifications promote subsequent S129 phosphorylation as part of a cellular control system, which contributes to the pathogenesis of the disease.

Results

α Syn forms dimers *in vivo*

Exposure of α Syn to nitrating agents causes tyrosine nitration *in vitro* and leads to formation of covalently crosslinked α Syn dimers and inclusions [42, 49, 50, 53, 56]. High levels of α Syn with C-terminal HIS₆-tags were heterologously expressed in yeast cells to uncover how nitration influences *in vivo* α Syn toxicity and aggregate formation.

The first approach was to examine whether α Syn and A30P form dimers *in vivo* without additional exposure of the cells to nitrating or oxidative agents. α Syn and A30P expression was driven by the *GALI*-promoter which was repressed in the presence of glucose and induced when shifted to 2% galactose-containing medium for 12 hours (h). High copy number expression of the HIS₆-tagged α Syn resulted in growth inhibition whereas high expression of the A30P mutant resulted in a similar growth rate as the yeast control without any α Syn (Fig 1A). Similar results were previously reported with untagged or GFP-tagged α Syn and corroborate that the HIS₆-tag does not interfere with the behavior of α Syn in yeast [60, 63]. α Syn proteins were enriched by Ni²⁺ pull-down under denaturing conditions in the presence of urea. Immunoblotting with anti- α Syn antibody revealed distinct bands, corresponding to monomeric (~17 kDa), dimeric (~35 kDa) and higher molecular weight α Syn species (oligomers), detected from *in vivo* samples (Fig 1B). This supports that α Syn and the A30P mutant form dimers and oligomers *in vivo* even without additional exposure of the cells to nitrating or oxidative agents.

Dimer and oligomer formation of α Syn *in vivo* was further analyzed by comparison to additional *in vitro* nitration [42]. PON (ONOO⁻) was applied as nitrating agent for α Syn tyrosine residues because it leads to the formation of stable α Syn oligomers. PON is formed by the reaction of superoxide ($\cdot\text{O}_2^-$) with the free radical nitric oxide ($\cdot\text{NO}$). PON represents a major nitrating agent that causes tissue injury in several neurological disorders [70, 71]. α Syn and A30P proteins were expressed in yeast, pulled-down using Ni²⁺ and exposed to PON. Immunoblotting of the *in vitro* nitrated proteins revealed that the abundance of dimers and oligomers was significantly increased with the same pattern as for *in vivo* isolated α Syn species (Fig 1B). The major distinct band corresponds to the α Syn dimer species.

Quantification of the dimer band intensities of *in vivo* isolated probes revealed that A30P forms approximately twice as many dimers relative to monomers as wild-type α Syn. *In vitro* nitration of α Syn and A30P increased the total amount of dimers (Fig 1C). However, the dimer to monomer ratios between α Syn and A30P were not changed when the *in vivo* samples were enhanced by additional *in vitro* nitration (Fig 1C).

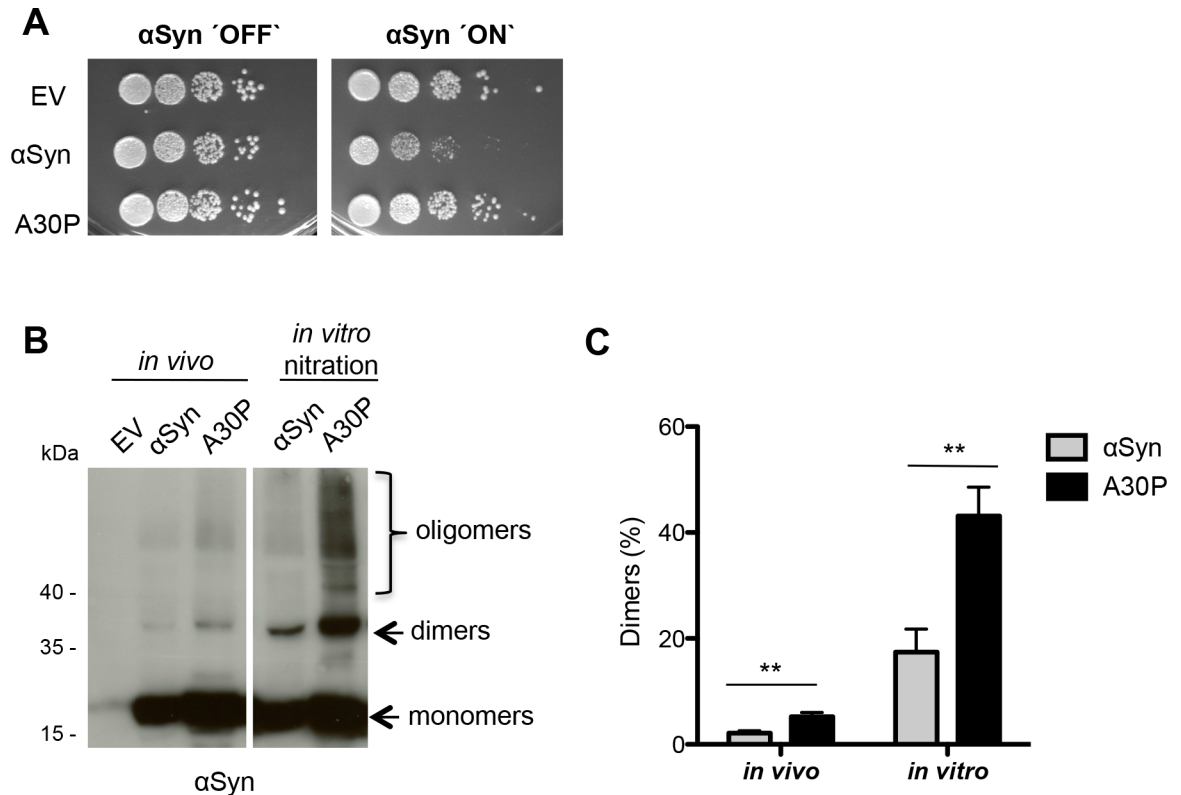


Fig 1. α Syn forms dimers *in vivo*. (A) Spotting analysis of yeast cells expressing C-terminally HIS₆-tagged α Syn and A30P α Syn on a high copy vector (2 μ) driven by the inducible GAL1-promoter on non-inducing ('OFF': glucose) and inducing ('ON': galactose) SC-Ura medium after 3 days. Control cells expressed only the empty vector pME2795 (EV). (B) Western blotting of α Syn and A30P enriched from cell extracts by Ni²⁺ pull-down with anti- α Syn antibody. *In vitro* nitration was carried out with 15 μ g of α Syn extracts using 1 μ l peroxyntirite (PON) in the presence of 1 μ l 0.3 M HCl. (C) Quantification of dimers. Densitometric analysis of the immunodetection of α Syn and A30P α Syn dimers *in vivo* and in PON-treated samples. The amount of dimers is presented as percent of the total amount of α Syn detected per lane (monomer + dimer). Significance of differences was calculated with t-test (**, $p < 0.01$, $n = 4$).

doi:10.1371/journal.pgen.1006098.g001

Our results suggest that the high molecular weight variants of α Syn, which can be isolated from yeast cells and which withstand strong denaturing conditions during the pull-down (8 M Urea, 2% SDS), represent covalently crosslinked α Syn species. These data support the formation of α Syn dimers in living cells. A remarkable result is that the toxicity of α Syn, which correlates to a high protein aggregation rate [63], results in a reduced amount of α Syn dimer relative to monomer formation. In contrast, the non-toxic A30P mutant that does not inhibit cellular growth (Fig 1A), and has a reduced aggregation rate, produces twice as many dimers relative to monomers in comparison to wild-type α Syn. This suggests that α Syn dimer formation is a molecular mechanism which can be used by the cell as salvage pathway for detoxification.

The C-terminus of α Syn is preferentially modified by nitration and di-tyrosine formation

Liquid chromatography–mass spectrometry (LC-MS) analysis was performed to analyze α Syn and A30P nitration sites *in vivo*. Single trypsin or AspN digestions were employed and the resulting peptides were analyzed by LC-MS. In addition to single digestions, a combined proteolytic approach by double digestion of the proteins with trypsin and AspN was employed that enabled 100% sequence coverage. The modifications of the tyrosine residues identified

	<i>in vivo</i>				<i>in vitro</i> (PON)			
	Y39	Y125	Y133	Y136	Y39	Y125	Y133	Y136
α Syn monomers		3-NT	3-NT	3-NT	3-NT	3-NT	3-NT	3-NT
α Syn dimers					3-NT			
A30P monomers		3-NT			3-NT	3-NT	3-NT	
A30P dimers					3-NT	3-NT	3-NT	

Fig 2. Determination of nitrated peptides from α Syn and A30P. α Syn and A30P were enriched by Ni²⁺ pull-down from yeast crude extracts and separated by SDS-PAGE. Monomeric and dimeric α Syn stained with Coomassie were excised from the gel and digested with trypsin and AspN. Untreated (*in vivo*) and subsequent peroxyxynitrite (PON) treated (*in vitro*) α Syn and A30P protein samples were analyzed with LC-MS for tyrosine nitration. 3-NT (3-nitrotyrosine) indicates identified nitration sites, supported by at least two peptides and two independent experiments.

doi:10.1371/journal.pgen.1006098.g002

from fragment spectra are summarized in Fig 2. MS data revealed nitration of wild-type α Syn at all three C-terminal tyrosines (Y125, Y133, Y136). Nitration of A30P was restricted to Y125 and absent at Y133 or Y136. Nitration of the additional tyrosine residue Y39 in the N-terminal domain of α Syn could not be identified from any *in vivo* samples by MS. Pull-down and additional PON exposure, however, resulted in Y39 nitration in all samples. This suggests that Y39 is not a primary *in vivo* nitration target within cells. Additional PON-exposure after pull-down also revealed that the α Syn dimers can be potentially nitrated *in vitro*. The increased *in vitro* PON-mediated nitration of the A30P in comparison to wild-type could be due to the higher amounts of the dimer in this mutant strain.

Beyond nitration we could also identify phosphorylation in α Syn as well as A30P at S129, Y125 or Y133 but not at Y39 or Y136 (Table 1). The probabilities for possible phosphorylation sites were calculated with the phosphoRS algorithm [72]. Phosphorylation of Y125 was identified with only low probability scores (Table 1). In contrast, S129 and Y133 were almost completely co-phosphorylated with scores of 100% for S129 and 99% for Y133, respectively.

The LC-MS spectra of α Syn and A30P migrating in SDS-PAGE with the size of the dimer band were analyzed to assess whether di-tyrosines cause dimer formation of α Syn or A30P. The presence of di-tyrosine peptide crosslinks was validated using StavroX2.3.4.5 software [73]. This software compares the masses of all potential crosslinked peptides with the precursor ion masses, calculates b- and y-type ions for all possible crosslinks and compares them to MS2 data of the precursor ion. Different combinations of crosslinked peptides with an identical mass are possible when multiple tyrosine residues are located on one and the same peptide.

Table 1. Phospho-peptides identified by MS/MS.

Position	Modification	PTM Score α Syn	PTM Score A30P	Sequence Motif
Y39	Phospho	0	1.5	KEGVLYVGSKT
Y125	Phospho	9.7	8	PDNEAYEMPSE
S129	Phospho	100	100	AYEMPS EEGYQ
Y133	Phospho	99.8	100	PSEEGYQDYEP
Y136	Phospho	0	0	EGYQDY EPEA

Posttranslational modification (PTM) scores were calculated with phosphoRS algorithm and represent the probability for phosphorylation modification. The corresponding amino acid is indicated by a small letter code in the sequence motif. Number of peptide sequence matches: α Syn = 332; A30P = 414.

doi:10.1371/journal.pgen.1006098.t001

The crosslinked tyrosine pairs were assigned according to the scores calculated by StavroX based on the fragment ion series of the MS2 spectra. The MS data analysis verified that α Syn dimers are crosslinked by tyrosine residues. The detected combinations of crosslinked tyrosines are depicted in Fig 3A. The results indicate a strong preference for crosslinking of defined combinations of tyrosines (Figs 3A, 3B, 3C and S1). The most frequent combinations for either wild-type α Syn or A30P are Y125-Y136 and Y133-Y136 dimers which are all located in the C-terminus. Only the C-terminal tyrosine residues can mutually interact. Only a small fraction of Y39-Y39 dimers were found and there are no tyrosine dimers between the N-terminal Y39 and the C-terminal tyrosines of α Syn or A30P.

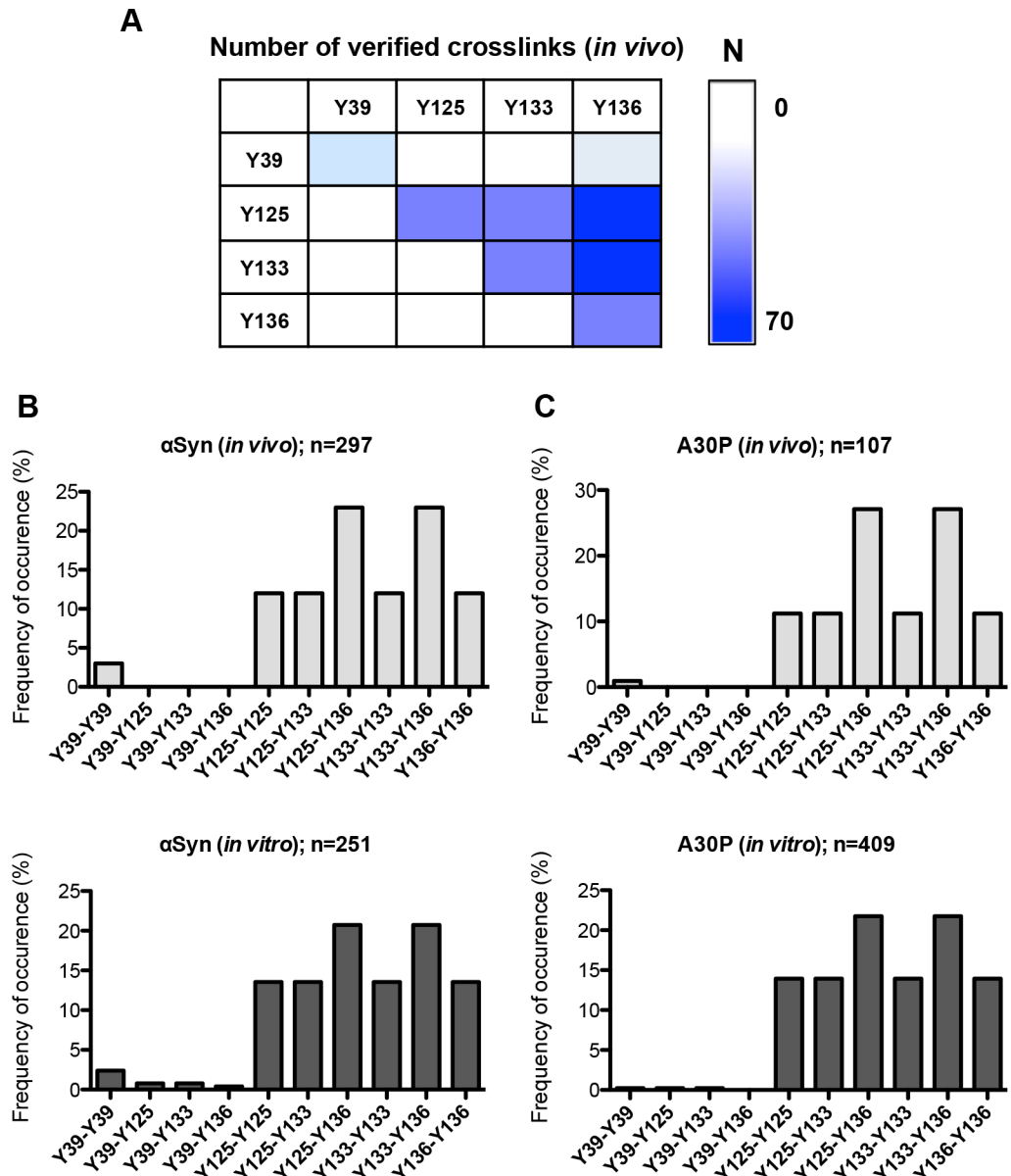


Fig 3. Determination of crosslinked peptides from α Syn and A30P. (A) Analysis of di-tyrosine dimers. Exemplary heat map diagram of the number (N) of identified di-tyrosine crosslinked peptides of the non-treated α Syn samples. (B) Distribution of all identified di-tyrosine peptides for α Syn. Identified combinations of crosslinked peptides are presented as percentage of n (n = total number of MS2 spectra verified as crosslinked peptides). (C) Distribution of all identified di-tyrosine peptides for A30P.

doi:10.1371/journal.pgen.1006098.g003

These data suggest that the C-terminus of α Syn or A30P has an increased susceptibility for nitration and di-tyrosine formation compared to the N-terminus. Only Y125 is a major nitration site of A30P. In contrast, all three C-terminal tyrosines Y125, Y133 and Y136 of the wild-type α Syn are putative targets for nitration. Y133 is an additional strong and Y125 a weak phosphorylation site, respectively. Dimer formation through di-tyrosine follows a specific pattern for both tested α Syn proteins with predominant forms including Y136 interacting either with Y125 (Y125-Y136) or with Y133 (Y133-136).

Tyrosine residues contribute to α Syn-mediated growth inhibition and aggregate formation

The codons for the four tyrosine sites of α Syn and A30P (Y39, Y125, Y133 and Y136) were replaced in the corresponding genes by phenylalanine codons (4(Y/F)) to analyze the role of the tyrosine residues on α Syn dimer formation, cytotoxicity or aggregation. Fusion genes with GFP-tags or HIS₆-tags were constructed and expressed. We assessed whether the quadruple Y to F replacements influence the dimerization of α Syn and A30P. Expression of α Syn and A30P as well as their 4(Y/F) mutants was induced for 12 h. Tagged proteins were enriched by Ni²⁺ pull-down under denaturing conditions. Immunoblotting using α Syn antibodies as well as antibodies that specifically recognize di-tyrosines revealed that 4(Y/F) mutants of α Syn or A30P had lost the potential to form dimers *in vivo* (Fig 4A). Additional *in vitro* nitration with PON did also not result in any dimer or oligomer formation and served as control (Fig 4A). Immunoblotting analysis was carried out to determine *in vivo* nitrated α Syn using 3-nitro-tyrosine specific antibodies (Fig 4B). The results demonstrated that the 4(Y/F) variants of wild-type α Syn or A30P did not result in any nitration signal even after additional PON treatment. This is in contrast to wild-type α Syn with its four original tyrosine residues as control where nitration is present *in vivo* and can be further increased by additional PON treatment.

The growth impact of wild-type α Syn or the A30P variant with that of the additional 4(Y/F) substitutions were compared by spotting analysis and in liquid medium, respectively (Fig 4C and 4D). Substitutions of the four tyrosine residues in wild-type α Syn significantly improved growth on solid medium, whereas A30P α Syn growth was similar with tyrosine or instead with phenylalanine residues (Fig 4C). Growth in liquid medium resulted in similar effects, revealing significantly reduced growth inhibition of the 4(Y/F) mutant strain in comparison to wild-type α Syn, whereas A30P and its A30P/4(Y/F) derivative were growing similarly (Fig 4D).

Next, we assessed whether the decrease in wild-type α Syn toxicity was related to the formation of α Syn inclusions (Fig 4E and 4F). No change in inclusion formation could be monitored when A30P was compared to A30P/4(Y/F). However, yeast cells expressing the 4(Y/F) α Syn variant formed less inclusions in comparison to wild-type α Syn (Fig 4E and 4F). Immunoblotting with α Syn antibody revealed that the protein levels of the different α Syn variants were similar (Fig 4G).

Taken together, only tyrosine replacements by phenylalanine in case of wild-type α Syn but not in case of an additional A30P substitution reduce α Syn-induced toxicity and inclusions formation. Accordingly, there is only growth improvement in the absence of an A30P substitution that correlates with decrease of intracellular accumulations of α Syn fluorescent foci. This supports that tyrosine residues that are responsible for nitration of α Syn contribute to the cytotoxic effect and inclusion formation of α Syn in yeast. This tyrosine-dependent effect is significantly less pronounced in the presence of an A30P codon mutation suggesting that A30P suppresses the tyrosine effect, which can be observed in wild-type α Syn. The presence of tyrosine residues in wild-type α Syn favor nitration and di-tyrosine-crosslinking but offer only a minor contribution to inclusion formation.

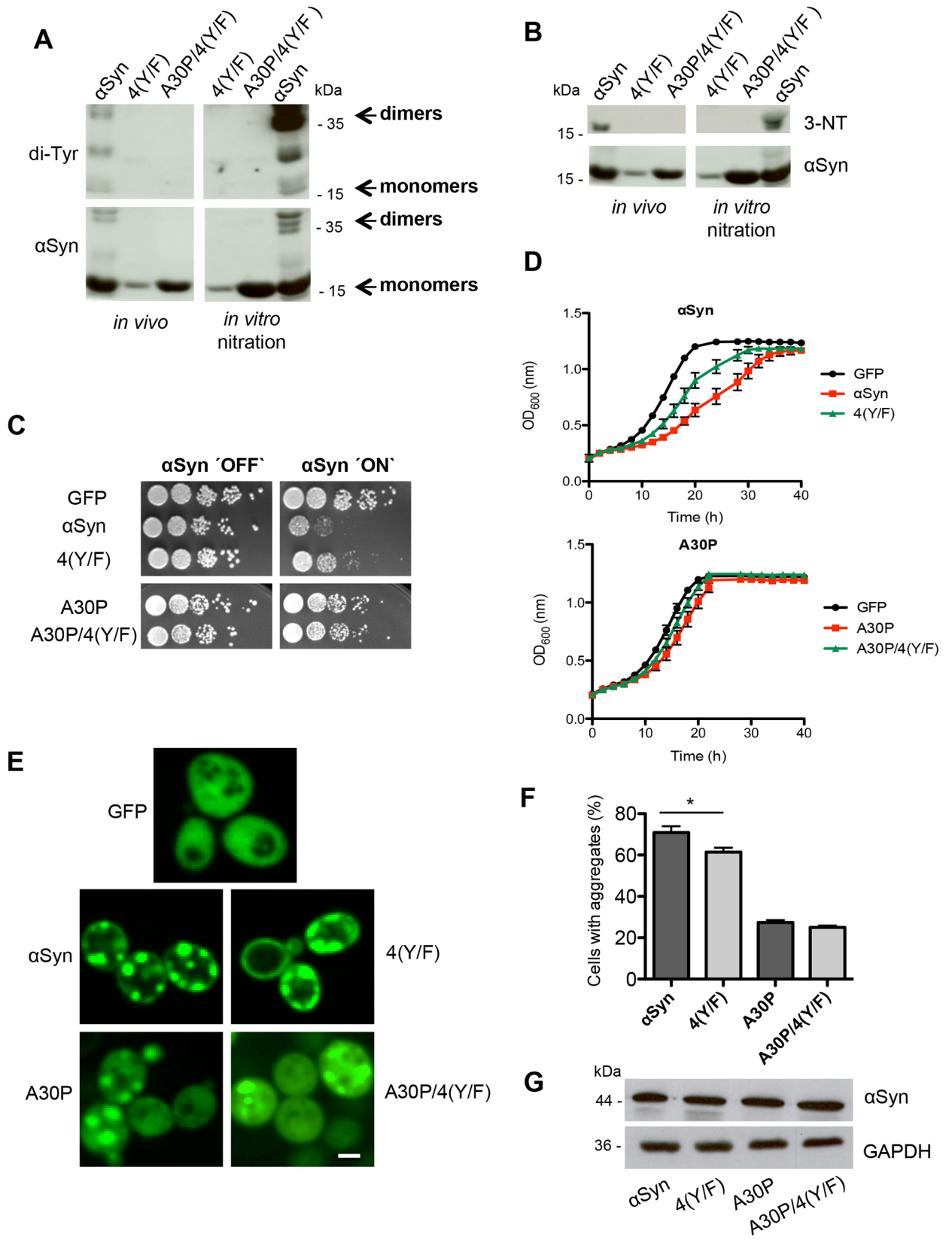


Fig 4. Blocking of α Syn tyrosine nitration decreases aggregation and cytotoxicity. (A) Expression of α Syn, A30P, 4(Y/F) and A30P/4(Y/F) α Syn was induced for 12 h in galactose-containing medium and the proteins were enriched by Ni^{2+} pull-down from yeast cell extracts. For *in vitro* nitration, 1 μl peroxyxynitrite (PON) was mixed with 15 μg of α Syn extracts in the presence of 1 μl 0.3 M HCl. Western blotting with di-tyrosine antibody reveals a major band at about 36 kDa, corresponding to dimers. Additional bands with lower molecular weights are observed, probably due to intramolecular di-tyrosine crosslinking. The same membrane was stripped and re-probed with α Syn antibody. (B) Western blotting using 3-nitro-tyrosine antibody (3-NT). Phenylalanine codon substitutions eliminate immunoreactivity. The same membrane was stripped and re-probed with α Syn antibody. (C) Spotting analysis of yeast cells expressing *GAL1*-driven α Syn, A30P, 4(Y/F), A30P/4(Y/F) α Syn and GFP (control). Yeast cells were spotted in 10-fold dilutions on SC-Ura plates containing glucose (α Syn 'OFF') or galactose (α Syn 'ON'). (D) Cell growth analysis of yeast cells expressing α Syn, A30P, 4(Y/F), A30P/4(Y/F) α Syn and GFP (control) in galactose-containing SC-Ura medium for 40 h. Error bars represent standard deviations of three independent experiments. (E) Fluorescence microscopy of yeast cells, expressing indicated α Syn-GFP variants after 6 h of induction in galactose-containing medium. Scale bar: 1 μm . (F) Quantification of the percentage of cells displaying aggregates after 6 h induction in galactose-containing medium. Significance of differences was calculated with t-test (*, $p < 0.05$, $n = 6$). (G) Western blotting analysis of protein crude extracts of GFP-tagged α Syn, 4(Y/F), A30P and A30P/4(Y/F) after 6 h induction in galactose-containing medium. GAPDH antibody was used as loading control.

doi:10.1371/journal.pgen.1006098.g004

The nitric oxide oxidoreductase Yhb1 reduces A30P aggregation and toxicity

The effect of nitrative stress on the toxicity and aggregation of wild-type and A30P mutant α Syn was examined. A yeast strain carrying a deletion in the yeast flavohemoglobin gene (*YHB1*), responsible for stress signaling, was used for enhancement of nitrative stress. Yhb1 is a nitric oxide oxidoreductase, which protects against nitration of cellular targets and against cell growth inhibition under aerobic or anaerobic conditions. Deletion of *YHB1* abolishes the nitric oxide (NO) consuming activity of yeast cells [74]. The compound DETA-NONOate causes nitrative stress by acting as a NO donor. The absence of the flavohemoglobin results in a growth impairment of the hypersensitive *yhb1* deletion strain in comparison to wild-type under NO nitrative stress conditions (Fig 5A).

The genes encoding wild-type or A30P α Syn, or GFP as a control, were expressed in $\Delta yhb1$ or the isogenic wild-type background. Cell growth was compared in the absence of nitrative stress by spotting assays (Fig 5B). Wild-type α Syn was as well cytotoxic in the presence or absence of *YHB1*. This was different for A30P, where no cytotoxicity was observed in the presence of *YHB1*. However, expression of A30P in $\Delta yhb1$ cells inhibited cell growth. This effect was verified by low copy plasmid expression of *YHB1*. Cells rescued with *YHB1* showed the same growth phenotype as the original A30P or the GFP control in the *YHB1* background (Fig 5B).

The correlation between growth inhibition and aggregate formation of α Syn variants was examined. Cells expressing α Syn or A30P were imaged by fluorescence microscopy and the cells displaying aggregates were counted. Deletion of *YHB1* resulted in increased percentage of cells with A30P inclusions, whereas no significant difference was observed in cell expressing wild-type α Syn (Fig 5C). In agreement with the growth analysis, the complementation of the $\Delta yhb1$ deletion by *YHB1* rescued the lower aggregation potential of A30P.

Deletion of *YHB1* constitutes an internal stress signal. The effect of nitrative stress on A30P was further investigated by adding external nitrative stress conditions. Growth tests in liquid culture were performed using DETA-NONOate, which reduces growth of the $\Delta yhb1$ mutant but not of the wild-type strain (Fig 5A). Cells expressing A30P α Syn grew uninhibited in the *YHB1* wild-type background, whereas $\Delta yhb1$ cells expressing A30P were less inhibited than α Syn, thus recapitulating the growth phenotype in solid medium (Fig 5B and 5D). In contrast, $\Delta yhb1$ cells expressing both α Syn variants were equally impaired in growth under nitrative stress conditions (Fig 5D). This indicates that increase in nitrative stress changes A30P to a toxic protein in yeast cells comparable to wild-type α Syn.

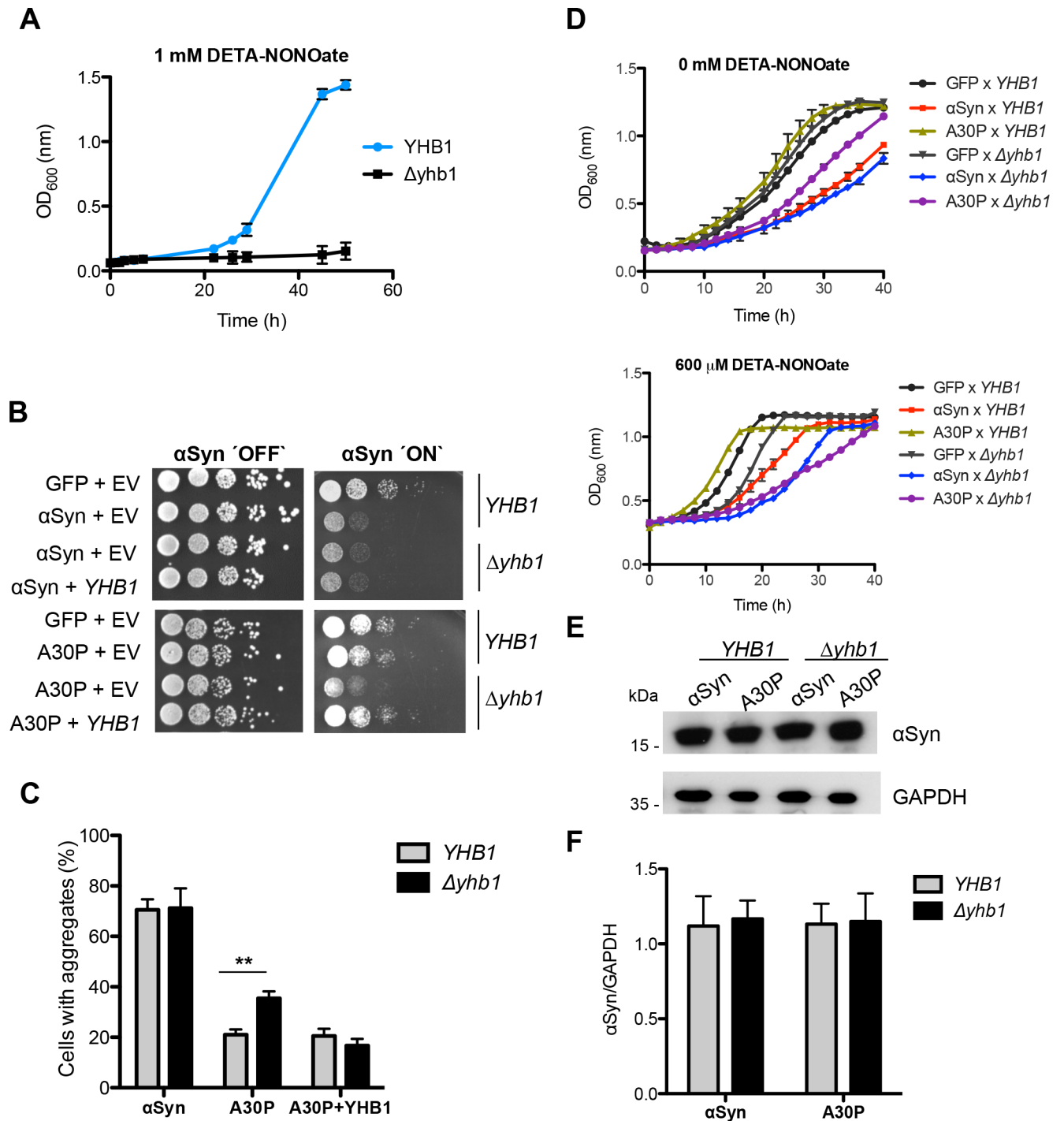


Fig 5. The nitric oxide oxidoreductase Yhb1 reduces A30P aggregation and toxicity. (A) Cell growth comparison of wild-type *YHB1* and mutant *$\Delta yhb1$* yeast cells in the presence of the NO stress-mediating drug DETA-NONOate (1 mM) in liquid galactose-containing SC-Ura medium. Error bars indicate standard deviations of three independent experiments. (B) Spotting analysis of *YHB1* and *$\Delta yhb1$* yeast cells expressing α Syn (upper boxes) or A30P (lower boxes) compared to GFP and empty vector (EV) as control on non-inducing and galactose-inducing SC-Ura medium after 3 days. (C) Quantification of the percentage of cells displaying α Syn aggregates after 6 h induction in galactose-containing medium. Significance of differences was calculated with t-test (**, $p < 0.01$, $n = 6$). (D) Cell growth analysis of *YHB1* and *$\Delta yhb1$* yeast cells expressing α Syn, A30P, 4(Y/F), A30P/4(Y/F) and GFP (control) after 40 h induction in galactose-containing SC-Ura medium. (upper panel, —DETA-NONOate; lower panel, + 600 μ M DETA-NONOate). Error bars show standard deviations of three independent experiments. (E) Western blotting analysis of protein crude extracts of α Syn and A30P expressed in *YHB1* and *$\Delta yhb1$* yeast after 6 h induction in galactose-containing medium. GAPDH antibody was used as loading control. (F) Quantification of α Syn and A30P levels in *YHB1* and *$\Delta yhb1$* yeast cells. Densitometric analysis of the immunodetection of α Syn and A30P relative to the intensity obtained for GAPDH ($n = 3$).

doi:10.1371/journal.pgen.1006098.g005

α Syn toxicity is dependent on the expression levels [60, 63]. Thus, it was tested whether the A30P expression level is equal in $\Delta yhb1$ mutant compared to *YHB1* yeast. Immunoblotting analysis revealed that the A30P variant was expressed at similar levels in both yeast backgrounds 6 h after induction of gene expression (Fig 5E and 5F), excluding that differences in toxicity are due to different A30P expression levels. These results suggest a specific suppressive function of the nitric oxide oxidoreductase Yhb1 on A30P-induced aggregate formation and growth inhibition in yeast.

Blockade of tyrosine nitration protects against A30P toxicity and aggregate formation under nitritive stress

The removal of the four tyrosines of α Syn as possible cellular nitration sites (4(Y/F)) might affect α Syn toxicity in yeast when the intracellular nitritive stress level is increased using a $\Delta yhb1$ strain defective in stress protection. This was examined by comparing α Syn, A30P and their 4(Y/F) derivatives which were expressed in yeast with wild-type *YHB1* or $\Delta yhb1$ deletion background.

Growth was analyzed by spotting analysis and in liquid medium (Fig 6A and 6B). Expression of 4(Y/F) α Syn with an intact *YHB1* gene resulted in improved growth, whereas A30P toxicity was not affected (Figs 6A, 6B, 4C and 4D). In the absence of the *YHB1* gene, A30P delayed growth. However, 4(Y/F) A30P grew similar to the GFP control. A30P-mediated toxicity was related to the formation of inclusions (Fig 6C).

These results corroborate that increased nitritive stress contributes to A30P toxicity by nitration of tyrosine residues. Nitration-deficient wild-type or A30P α Syn were less toxic and aggregated less, whereas an increase of intracellular nitritive stress resulted in growth retardation and increased aggregate formation of A30P variant only when tyrosine residues were present.

Yhb1 reduces the accumulation of reactive nitrogen species in A30P expressing yeast cells

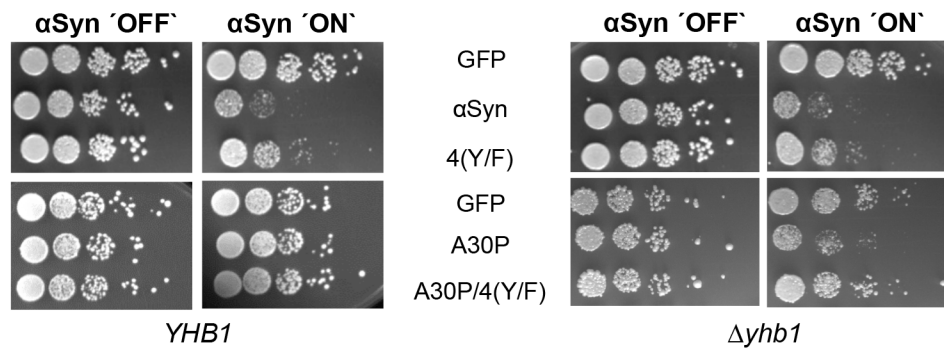
Oxidative and nitritive stresses are implicated in the pathogenesis of PD [75, 76]. These stresses emerge from the accumulation of reactive intermediates such as ROS and RNS. ROS and RNS production were visualized in yeast cells. α Syn and A30P expression was induced for 6 h and ROS and RNS specific dyes were applied to compare the production of the reactive species in *YHB1* and $\Delta yhb1$ cells by fluorescence microscopy and flow cytometry.

Dihydrorhodamine 123 (DHR123) was used for ROS detection. The dye accumulates in cells, where it is oxidized by free radicals to the bright red fluorescent product rhodamine 123 (Fig 7A–7C). Expression of A30P and its derivative A30P/4(Y/F) did not significantly increase the number of cells accumulating ROS. In contrast, expression of wild-type α Syn as well as its 4(Y/F) derivative strongly increased the number of cells that accumulate red fluorescence indicative for ROS (Fig 7C). No difference in ROS accumulation was observed between the *YHB1* wild-type and the $\Delta yhb1$ mutant strain.

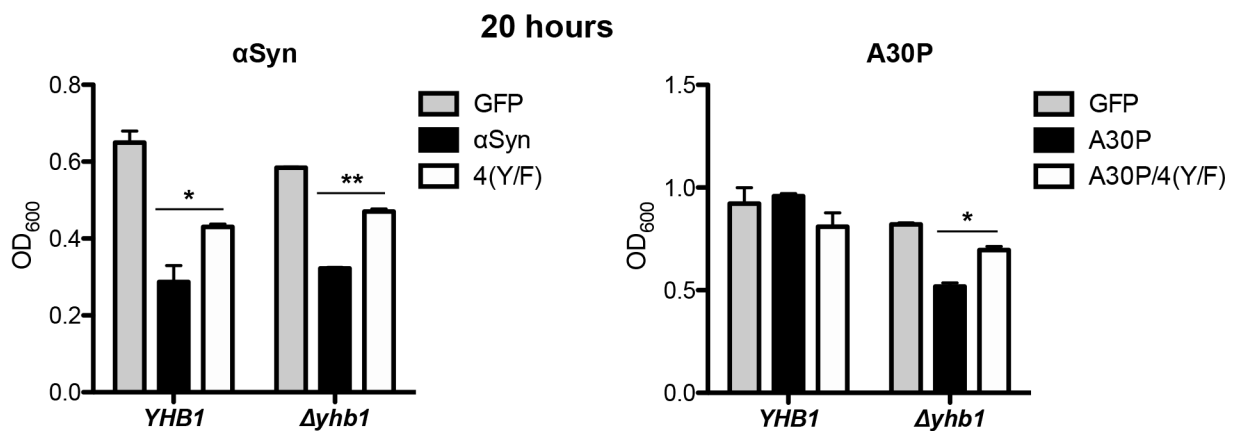
DAF-2 DA (4,5-Diaminofluorescein diacetate) dye was used as a sensitive and highly specific fluorescent indicator for detection of NO (Fig 7D–7F). Expression of both α Syn and A30P induced accumulation of reactive nitrogen species (Fig 7F). Interestingly, deletion of *YHB1* significantly increased the number of cells exhibiting RNS when A30P variant was expressed. This effect was dependent on tyrosine residues since RNS accumulation in cells expressing A30P/4(Y/F) did not differ from empty vector control.

The results show that toxic wild-type α Syn expression induces significantly more ROS accumulation in yeast cells than non-toxic A30P. Accumulation of ROS species was not dependent

A



B



C

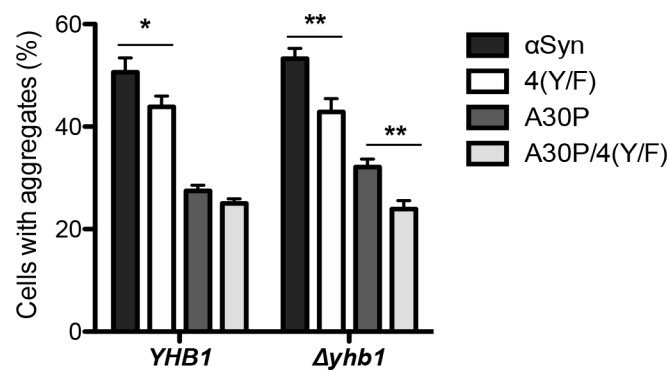


Fig 6. Tyrosine mutation of A30P decreases toxicity in $\Delta yhb1$. (A) Spotting analysis of α Syn, A30P, 4(Y/F) α Syn, A30P/4(Y/F) and GFP (control) expressed in *YHB1* and $\Delta yhb1$ yeast on non-inducing and galactose-inducing SC-Ura plates after 3 days of growth. (B) Cell growth analysis of *YHB1* and $\Delta yhb1$ yeast expressing α Syn, A30P, 4(Y/F), A30P/4(Y/F) and GFP (control) at time point 20 h. Significance of differences was calculated with t-test (*, $p < 0.05$; **, $p < 0.01$, $n = 3$). (C) Quantification of the percentage of cells displaying α Syn aggregates after 6 h induction in galactose-containing SC-Ura medium. Significance of differences was calculated with t-test (*, $p < 0.05$, **, $p < 0.01$, $n = 6$).

doi:10.1371/journal.pgen.1006098.g006

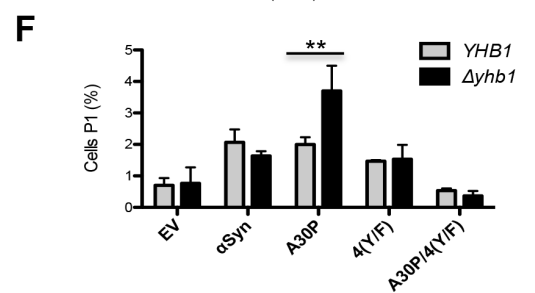
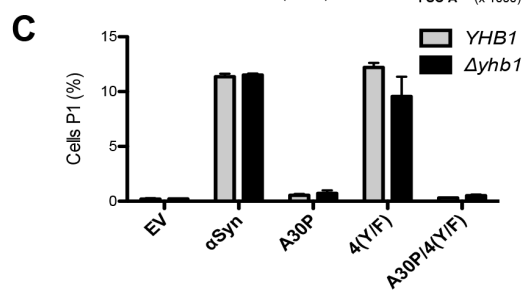
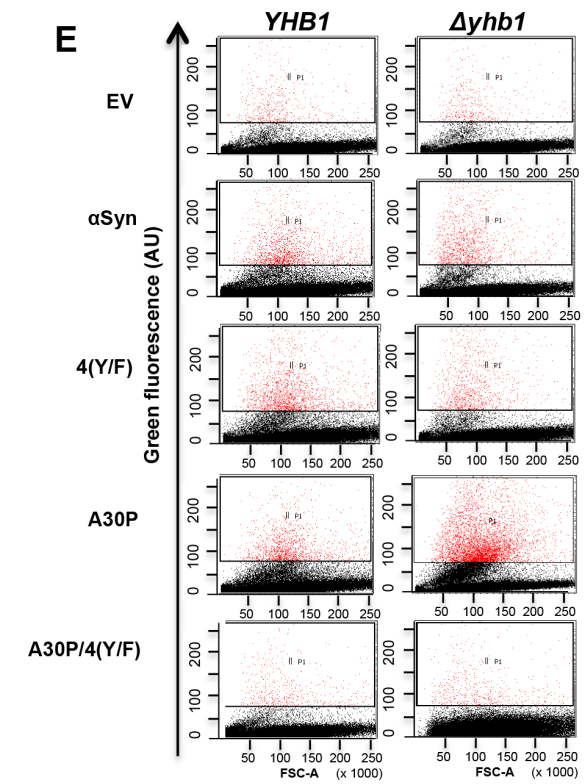
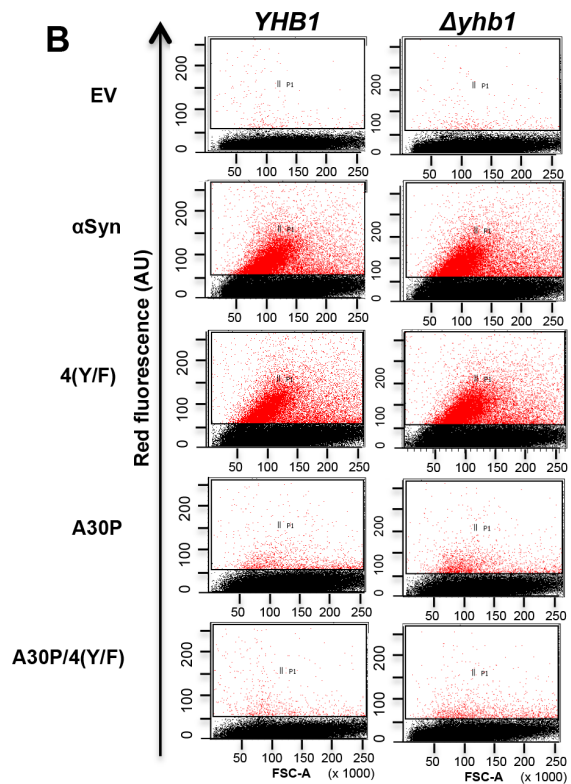
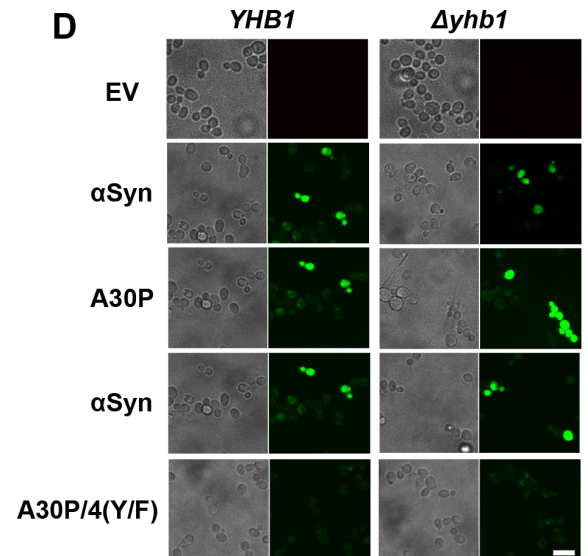
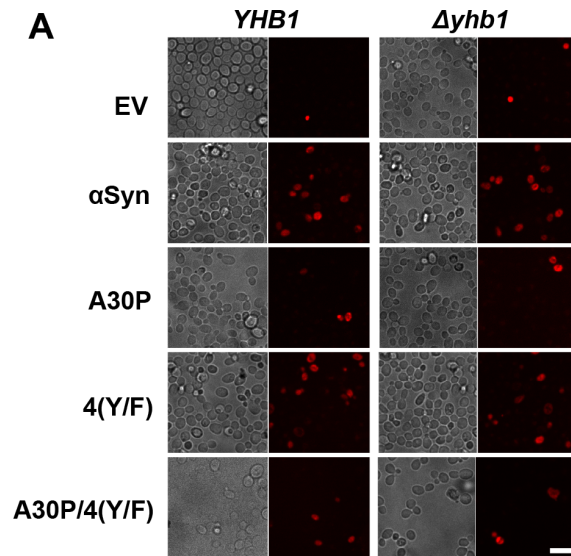


Fig 7. *YHB1* deletion increases accumulation of reactive nitrogen species (RNS) in A30P expressing cells. (A) α Syn, A30P, 4(Y/F) and A30P/4(Y/F) were induced in galactose-containing medium for 6 h in *YHB1* wild-type or $\Delta yhb1$ deletion yeast strains. Cells were incubated with dihydrorhodamine 123 (DHR123) as an indicator of high intracellular ROS accumulation for 1.5 h and analyzed by live-cell fluorescence microscopy. Scale bar = 5 μ m. (B) Fluorescent intensity of cells from (A), assessed with flow cytometry analysis. Forward scatter (FSC) and DHR123 fluorescence of cells after 6 h induction of α Syn expression. (C) Quantification of α Syn, A30P, 4(Y/F) and A30P/4(Y/F) expressing cells displaying ROS stained by DHR123 using flow cytometry. The percentage of the sub-population of yeast cells with higher fluorescent intensities (P1) than the background is presented. (D) Microscopy analysis of RNS stained cells. α Syn, A30P, 4(Y/F) and A30P/4(Y/F) were induced in galactose-containing SC-Ura medium for 6 h in *YHB1* and $\Delta yhb1$ yeast strains. Cells were incubated with DAF-2 DA for 1 h at 30°C for visualization of RNS and analyzed by live-cell fluorescence microscopy. Scale bar = 5 μ m. (E) Fluorescent intensity of cells from (D), assessed with flow cytometry analysis. Forward scatter (FSC) and DAF-2 DA fluorescence of cells after 6 h induction of α Syn expression. (F) Quantification of α Syn, A30P, 4(Y/F) and A30P/4(Y/F) expressing cells displaying RNS stained by DAF-2 DA using flow cytometry. The percentage of the sub-population of yeast cells with higher fluorescent intensities (P1) than the background is presented. Significance of differences was calculated with t-test (**, $p < 0.01$, $n = 3$).

doi:10.1371/journal.pgen.1006098.g007

on the presence of tyrosine residues or *YHB1* gene. In contrast, both α Syn as well as A30P induce the accumulation of RNS for oxidative stress in yeast cells. The levels of RNS in A30P but not wild-type α Syn expressing cells are dependent on the presence of tyrosine residues and *YHB1*. The results suggest that Yhb1 attenuates the accumulation of RNS of A30P expressing cells.

Yhb1 protects mitochondria from A30P-mediated toxicity

Overexpression of α Syn and A30P leads to increased levels of RNS and higher sensitivity to NO stress in $\Delta yhb1$ yeast. The Yhb1 protein is translocated into yeast mitochondria under hypoxic conditions where it detoxifies NO [77]. Mitochondria are a major source of free radicals in the cells. Yhb1 is consuming NO, which inhibits mitochondrial respiration and thus increases the level of ROS. α Syn toxicity results in mitochondrial dysfunction and generation of ROS [65]. Overexpression of α Syn in mammalian cells results in mitochondrial fragmentation and involves a direct interaction of α Syn with mitochondrial membranes [78].

We examined whether deletion of *YHB1* influences the mitochondrial morphology in α Syn and A30P α Syn expressing yeast cells. α Syn expression in the wild-type and $\Delta yhb1$ background was induced for 6 h in galactose medium and the mitochondria were visualized with a mitochondrial specific dye (MitoTracker Red). Cells expressing GFP were used as a control (Fig 8A). We could not detect co-localization of α Syn with mitochondria, which suggests that the described mitochondrial fraction of the protein might be small [78]. The mitochondrial morphology was classified as tubular, partially fragmented or fully fragmented. In the control cells, the mitochondria revealed a ribbon-like tubular architecture, typical for healthy mitochondria. Cells expressing α Syn showed a dramatic increase in the percentage of cells with fully fragmented mitochondria (Fig 8A and 8B). Cells with and without inclusions were considered separately for statistical evaluation. Cells with plasma-membrane localization of the GFP-signal, typical α Syn localization for early stages of expression or lower expression levels, revealed partially fragmented mitochondrial architecture. α Syn expressing cells with aggregates had fully fragmented mitochondria. In contrast to α Syn, A30P expressing cells with aggregates had mainly tubular mitochondria, similar to the control cells (Fig 8A). Deletion of *YHB1* increased the percentage of cells with fully fragmented mitochondria almost two-fold (Fig 8B). Thus, the disrupted mitochondrial morphology in $\Delta yhb1$ correlates with the increased levels of RNS (Fig 7D–7F) and diminished growth behavior of A30P expressing cells (Fig 5B and 5D). Complementation of the $\Delta yhb1$ phenotype in A30P expressing cells rescued the defect (Fig 8C), as mitochondrial morphology was recovered by expression of *YHB1* on a low-copy vector. The result suggests that Yhb1 protects against A30P-induced cytotoxicity by preventing the mitochondrial fragmentation.

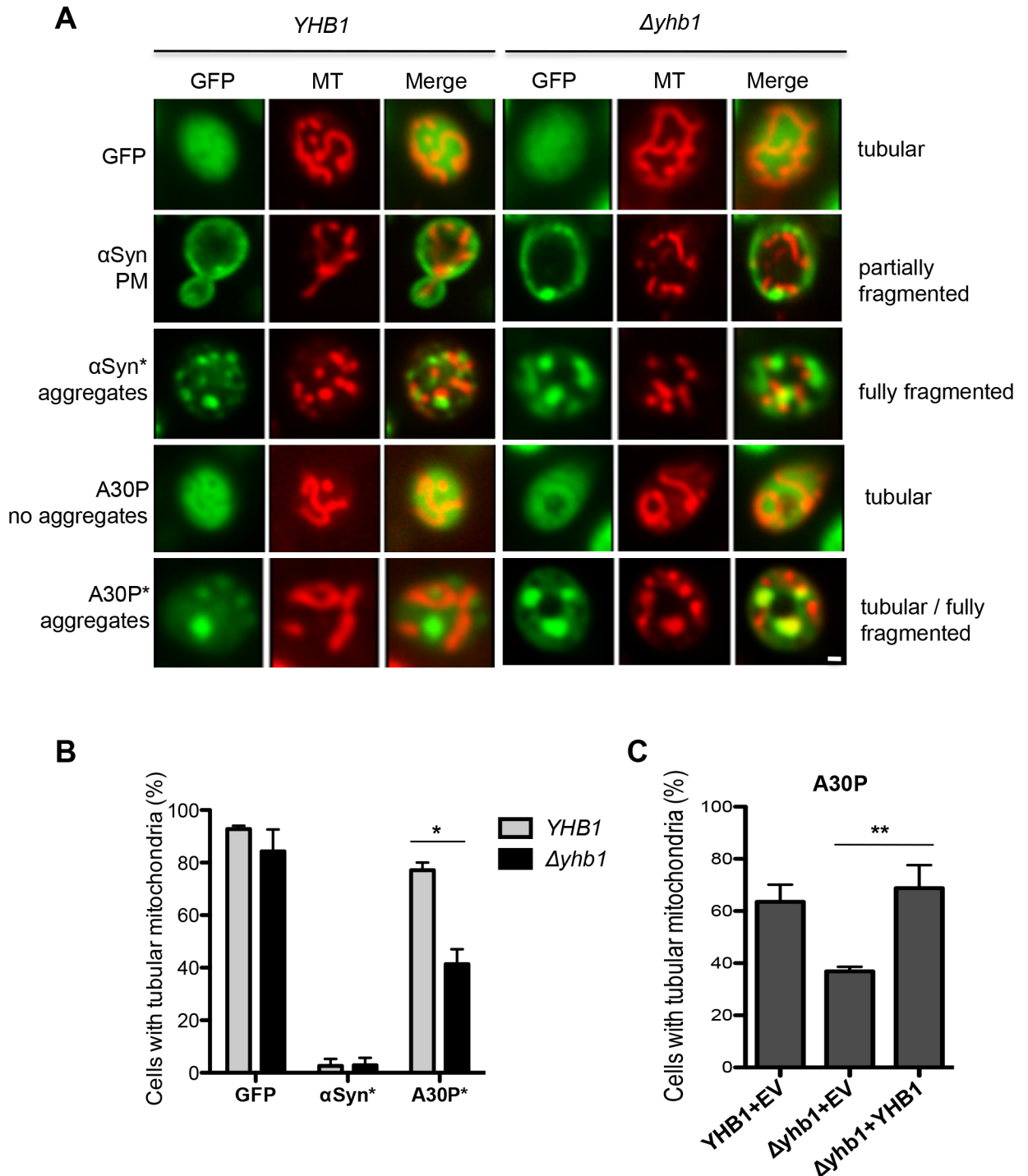


Fig 8. Yhb1 protects mitochondria from A30P toxicity. (A) Live-cell fluorescence microscopy of *YHB1* compared to $\Delta yhb1$ yeast cells expressing GFP (control), α Syn or A30P after 6 h induction in galactose-containing medium. MitoTracker Red was used to visualize mitochondria in the cells (MT panel). α Syn expressing cells with plasma membrane localization (PM) and with aggregates are visualized. Scale bar = 1 μ M. (B) Quantification of yeast cells with tubular mitochondrial network. GFP: percentage of all cells with tubular mitochondria; α Syn* and A30P*: percentage of cells with aggregates, showing tubular mitochondria. At least 50 cells were counted per cell type and experiment. Significance of differences was calculated with t-test (*, $p < 0.05$, $n = 4$). (C) Quantification of yeast cells with tubular mitochondrial network for rescue of A30P phenotype. A30P with empty vector (EV) in *YHB1* and $\Delta yhb1$ strain and A30P co-transformed with *YHB1* on low-copy vector in $\Delta yhb1$ strain. A30P*: percentage of cells with aggregates, showing tubular mitochondria. Significance of differences was calculated with t-test (**, $p < 0.01$, $n = 3$).

doi:10.1371/journal.pgen.1006098.g008

Human neuroglobin protects against α Syn aggregate formation in yeast and in mammalian cells

A BLAST search for human genes corresponding to yeast *YHB1* revealed 49% similarities of the *YHB1* globin domain to human neuroglobin (*NGB*) as a putative homolog. We analyzed whether the human counterpart of yeast *YHB1* can affect α Syn aggregation. Neuroglobins are oxygen-binding proteins that are highly conserved among vertebrates and are expressed in the central and peripheral nervous system. They provide protection against hypoxic induced cell injury in the brain, which is associated with ROS and RNS accumulation [79]. Both Yhb1 and neuroglobin contain a globin domain and are members of the globin gene family. *NGB* was shown to diminish beta-amyloid-induced neurotoxicity *in vitro* and to attenuate the phenotypes in a transgenic mouse model of Alzheimer's disease [80] and to act as an oxidative stress-responsive sensor for neuroprotection [81]. Here we examined, whether human *NGB* affects α Syn or A30P growth and aggregate formation in yeast. Growth and aggregation of α Syn was not changed by the expression of the human *NGB* (Fig 9A and 9B). However, *NGB* expression in $\Delta yhb1$ deletion strain rescued A30P yeast growth (Fig 9C) and reduced the number of cells with A30P aggregates (Fig 9D). The effect of *NGB* in yeast is similar to the impact of *YHB1* on α Syn and A30P growth and aggregate formation (Fig 5C).

Next, we examined whether *NGB* has not only a protective role against α Syn aggregate formation in yeast but also in mammalian cells. Human Neuroglioma cells (H4) served as established α Syn aggregation model, where aggregation of α Syn is induced by co-expressing C-terminally modified α Syn (SynT) and synphilin-1, α Syn-interacting protein that was also found in LBs [61, 82]. H4 cells were co-transfected with SynT, synphilin-1 and *NGB* or empty vector and aggregate formation of SynT was monitored (Fig 9E and 9F). Expression of *NGB* reduced the number of cells with aggregates almost two-fold in comparison to the control and reduced the number of aggregates per cell. Lactate dehydrogenase (LDH) measurements were performed to determine, whether there is an effect of *NGB* on cell toxicity. LDH release into the cell culture medium is an indicator of damages of the plasma membrane and is used as cytotoxicity marker. LDH measurements were similar for all tested H4 cells and support that *NGB* does act as suppressor of α Syn aggregation without significantly causing cytotoxicity.

Yhb1 affects nitration but not dimerization level of α Syn and A30P

We assessed whether the different cytotoxicity of α Syn and A30P in yeast correlates with different nitration levels of the two variants in wild-type yeast background and under increased nitrate stress in $\Delta yhb1$ strain. Immunoblotting analysis performed with two specific antibodies against nitro-tyrosine (3-nitrotyrosine and nitro-Y39 α Syn) showed that α Syn and A30P are nitrated in the *YHB1* as well as in $\Delta yhb1$ yeast (Fig 10A). Quantification of band intensities of both nitrated α Syn variants revealed significantly higher nitration level of α Syn in comparison to A30P. Deletion of *YHB1* resulted in increase of A30P nitration level, whereas α Syn nitration level was not affected (Fig 10B). The increased nitration level does not correlate with an increased dimerization level of both α Syn variants. The dimerization was not influenced by nitrate stress enhancement (Fig 10C and 10D). The results suggest that nitration of α Syn contributes to the cytotoxicity of the protein, whereas dimer formation is in reverse correlation to toxicity.

Tyrosine 133 is required for phosphorylation of α Syn at serine 129

Phosphorylation of Y125 is required *in vitro* as a priming event for efficient phosphorylation of S129 by casein kinase CK1 [83]. Phosphorylation of S129 is the major PTM of α Syn, found in

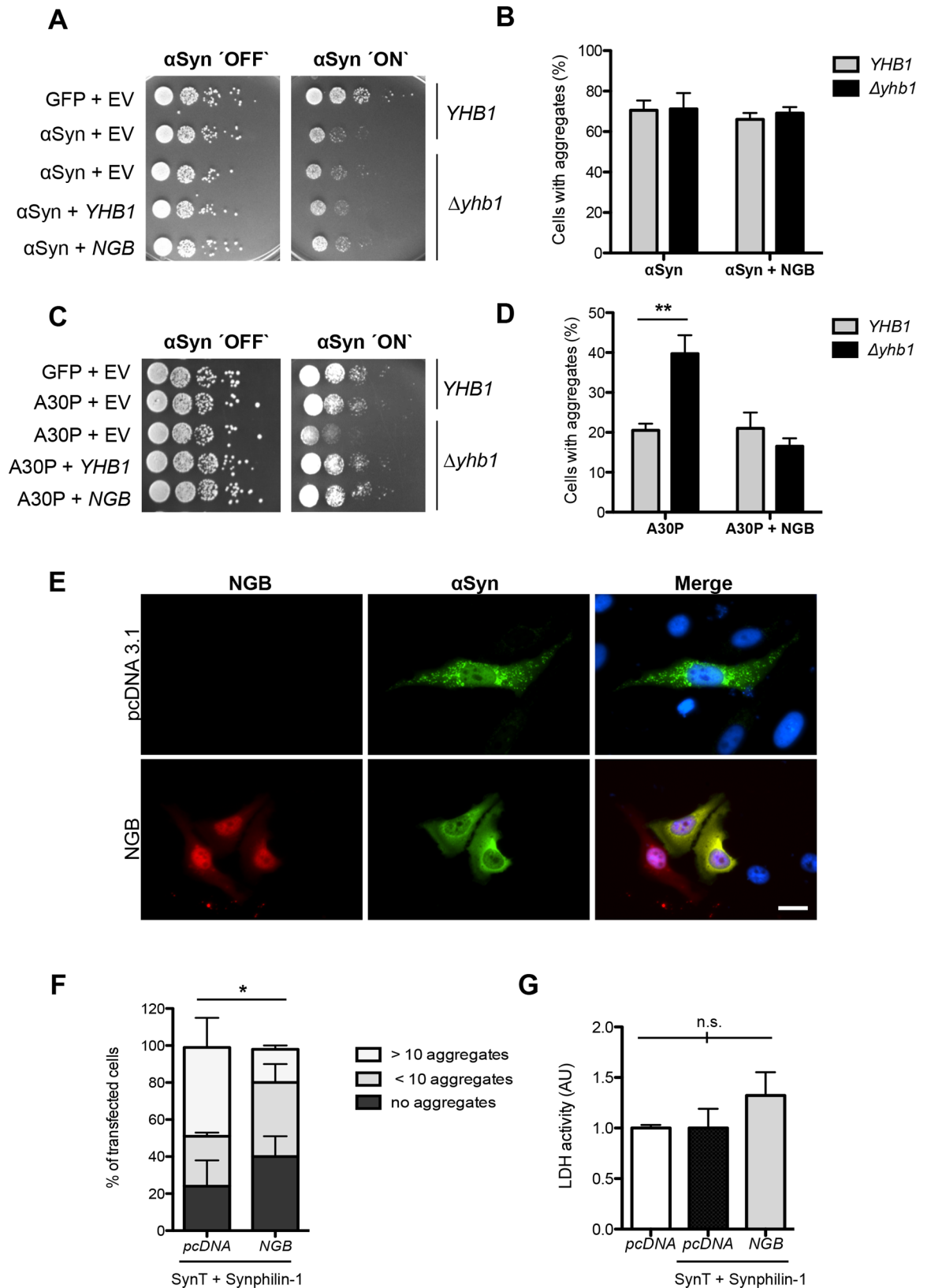


Fig 9. The human NGB gene for neuroglobin alters A30P and α Syn aggregation in yeast and mammalian cells. (A) Spotting analysis of YHB1 and $\Delta yhb1$ yeast cells co-expressing α Syn and GFP (control) with either empty vector as control or

YHB1 and *NGB*, respectively, on non-inducing and galactose-inducing SC-Ura medium after 3 days. (B) Quantification of the percentage of cells displaying α Syn aggregates after 6 h induction in galactose-containing medium ($n = 3$). (C) Spotting analysis of *YHB1* and *Δyhb1* yeast cells co-expressing A30P and GFP (control) with either empty vector (pME2788) as control or *YHB1* and *NGB*, respectively, on non-inducing and galactose-inducing SC-Ura medium after 3 days. (D) Quantification of the percentage of cells displaying A30P aggregates after 6 h induction in galactose-containing medium. Significance of differences was calculated with t-test (**, $p < 0.01$, $n = 3$). (E) Fluorescence microscopy of H4 cells co-expressing SynT, synphilin-1 and pcDNA (control) or *NGB*-mCherry. Nuclei are stained with Hoechst dye (blue). Scale bar = 30 μ m. (F) Quantification of the percentage of H4 cells displaying α Syn inclusions after 48 h after transfection. Cells were classified into three groups according to the number of α Syn-immunoreactive inclusions observed: cells with 10 inclusions, cells with less than 10 inclusions and cells without inclusions. Significance of differences was calculated with t-test (*, $p < 0.05$, $n = 3$). (G) Lactate dehydrogenase (LDH) activity measurements support that *NGB* is non-toxic for H4 cells. H4 cells transfected with empty mammalian expression vector pcDNA3.1, with empty pcDNA3.1 or pcDNA3.1 encoding neuroglobin-mCherry (*NGB*) together with SynT and synphilin-1 (SynT+Synphilin-1) were analyzed. Media from indicated H4 cells were collected and the secretion of lactate LDH was determined as a measure of cytotoxicity. Significance of differences was calculated with t-test (not significant (n.s.); $n = 3$).

doi:10.1371/journal.pgen.1006098.g009

90% of the aggregated protein in neuronal inclusions of PD patients [37]. α Syn and A30P are phosphorylated at S129 in yeast by endogenous kinases and phosphorylation has a protective role against α Syn-induced toxicity and aggregate formation [39, 41]. Given the importance of these PTM and the close proximity of serine and tyrosine residues at the C-terminus, we assessed whether there is a cross-talk between modifications of tyrosine residues and phosphorylation of α Syn at S129 *in vivo*.

Immunoblotting with an antibody that specifically recognizes α Syn phosphorylated at Y133 showed that both α Syn and A30P are phosphorylated at these residues, in accordance with our results from MS analysis (Fig 11A). Quantification of Y133 phosphorylation revealed similar phosphorylation level of α Syn and A30P variant both in presence and absence of *Yhb1* (Fig 11B). We analyzed whether there is a difference between S129 phosphorylation level of α Syn and A30P. S129 phosphorylation level of α Syn was much higher than that of A30P (Fig 11A and 11B). Tyrosine to phenylalanine (Y/F) substitutions were analyzed for their effects on the phosphorylation level at S129. Y/F mutation of the N-terminal tyrosine 39 as well as of the C-terminal Y125 and Y136 did not affect the phosphorylation status of S129. In contrast, mutation of Y133 had a drastic impact and resulted in complete loss of phosphorylation at S129 (Fig 11C). Yeast growth was compared in spotting assay as well as in liquid culture between yeast cells, expressing Y/F single mutants and S129A phosphorylation deficient mutant (Fig 11D and 11E). Yeast growth was measured after 20 h induction of protein expression. Expression of Y133F resulted in significant growth inhibition in comparison with α Syn and other tyrosine mutants. S129A showed slight growth inhibition (Fig 11D and 11E) and significant increase in the number of cells with aggregates (Fig 11E). In addition to growth analysis, membrane integrity of the Y/F single mutants and S129A phosphorylation deficient mutant was examined to assess the cell viability of the mutants (Fig 11G and S2 Fig). Propidium iodide (PI) staining was used after 20 h of protein induction as a sensitive method to determine the fraction of cells with compromised membrane integrity. Expression of Y133F and S129A significantly diminished membrane integrity, corroborating that expression of these mutants results in increased cytotoxicity.

Flow cytometry measurements were performed to determine the accumulation of ROS and RNS in yeast cells, expressing the single mutants. DHR123 was used for detection of ROS (Fig 12A) and DAF-2 DA was used for detection of RNS (Fig 12B). Expression of all mutants revealed a significant increase in the levels of ROS and RNS in comparison with the control; however, no significant differences were observed between the single mutants revealing that the enhanced toxicity of Y133F and S129A mutant is not due to higher accumulation of ROS or RNS.

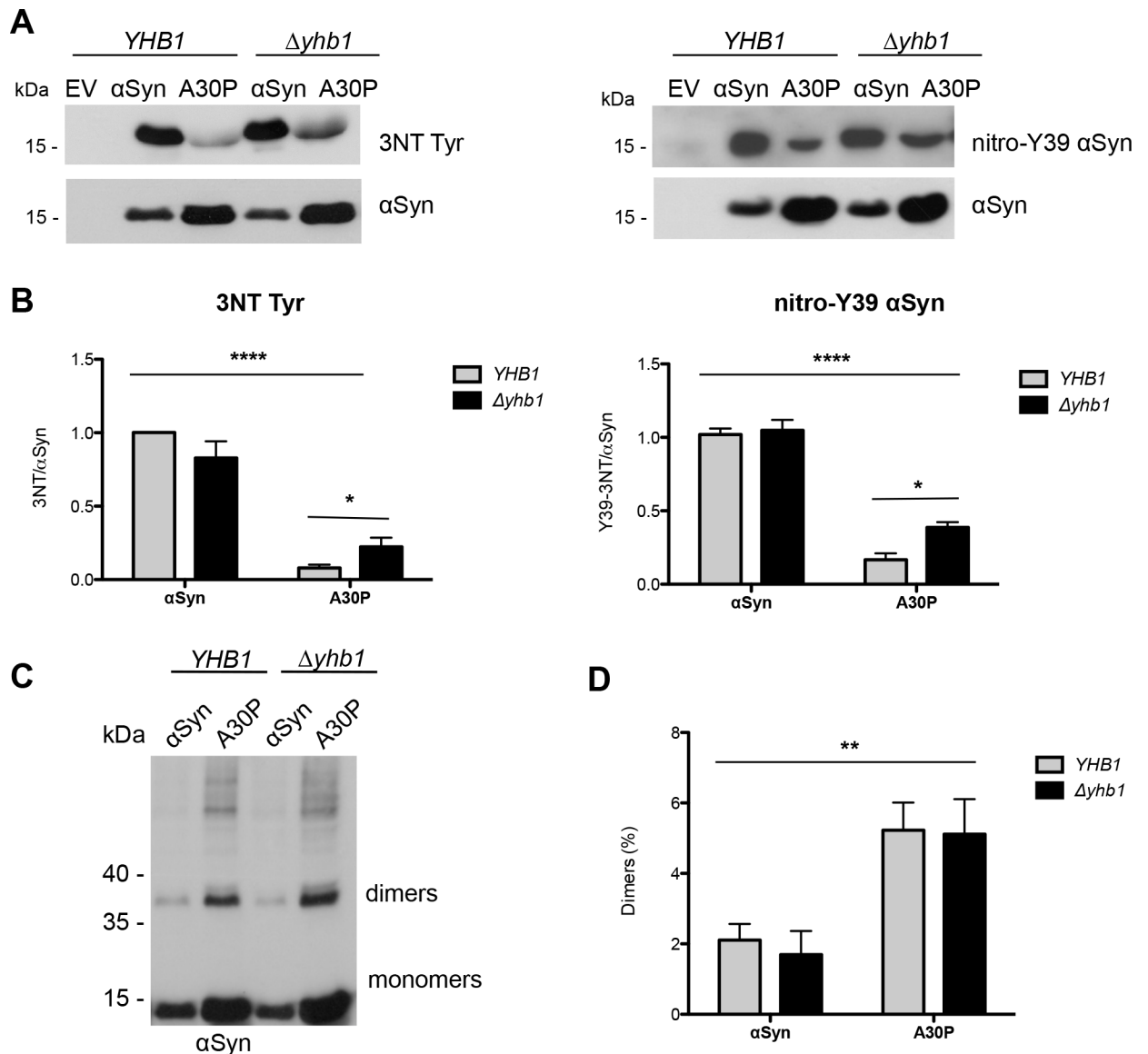


Fig 10. Yhb1 affects nitration but not dimerization of α Syn and A30P. (A) Immunoblotting analysis of 3-nitrotyrosine using 3-nitrotyrosine antibody (left) and nitro-Y39 α Syn antibody (right). Protein expression was induced for 12 h in galactose-containing SC-Ura medium. Concentrated protein extracts of Ni^{2+} pull down-enriched α Syn and A30P α Syn from YHB1 and $\Delta yhb1$ yeast cells were applied. Cells expressing empty vector (EV) served as control. The same membranes were stripped and re-probed with α Syn antibody. (B) Quantification of α Syn and A30P nitration levels in YHB1 and $\Delta yhb1$ yeast cells. Densitometric analysis of the immunodetection of nitrated α Syn and A30P relative to the intensity obtained for α Syn. Significance of differences was calculated with one-way ANOVA with Bonferroni's multiple comparison test (*, $p < 0.05$; ****, $p < 0.0001$; $n = 3$). (C) Western blotting of α Syn enriched by Ni^{2+} pull-down with α Syn antibody. (D) Ratio of dimers relative to the sum of monomers and dimers. Densitometric analysis of the immunodetection of α Syn and A30P α Syn dimers, presented as percent of the total amount of α Syn detected per lane (monomer + dimer). Significance of differences was calculated with one-way ANOVA (**, $p < 0.01$; $n = 4$).

doi:10.1371/journal.pgen.1006098.g010

These results indicate that Y133 is required for the protective effect of α Syn S129 phosphorylation *in vivo*. Expression of Y133F was more toxic than expression of S129A phosphorylation deficient mutant, suggesting additional protective contribution of Y133 modifications against α Syn cytotoxicity. The data support a complex cross-talk between nitration and phosphorylation of the C-terminal tyrosine residues and S129 phosphorylation of α Syn and A30P.

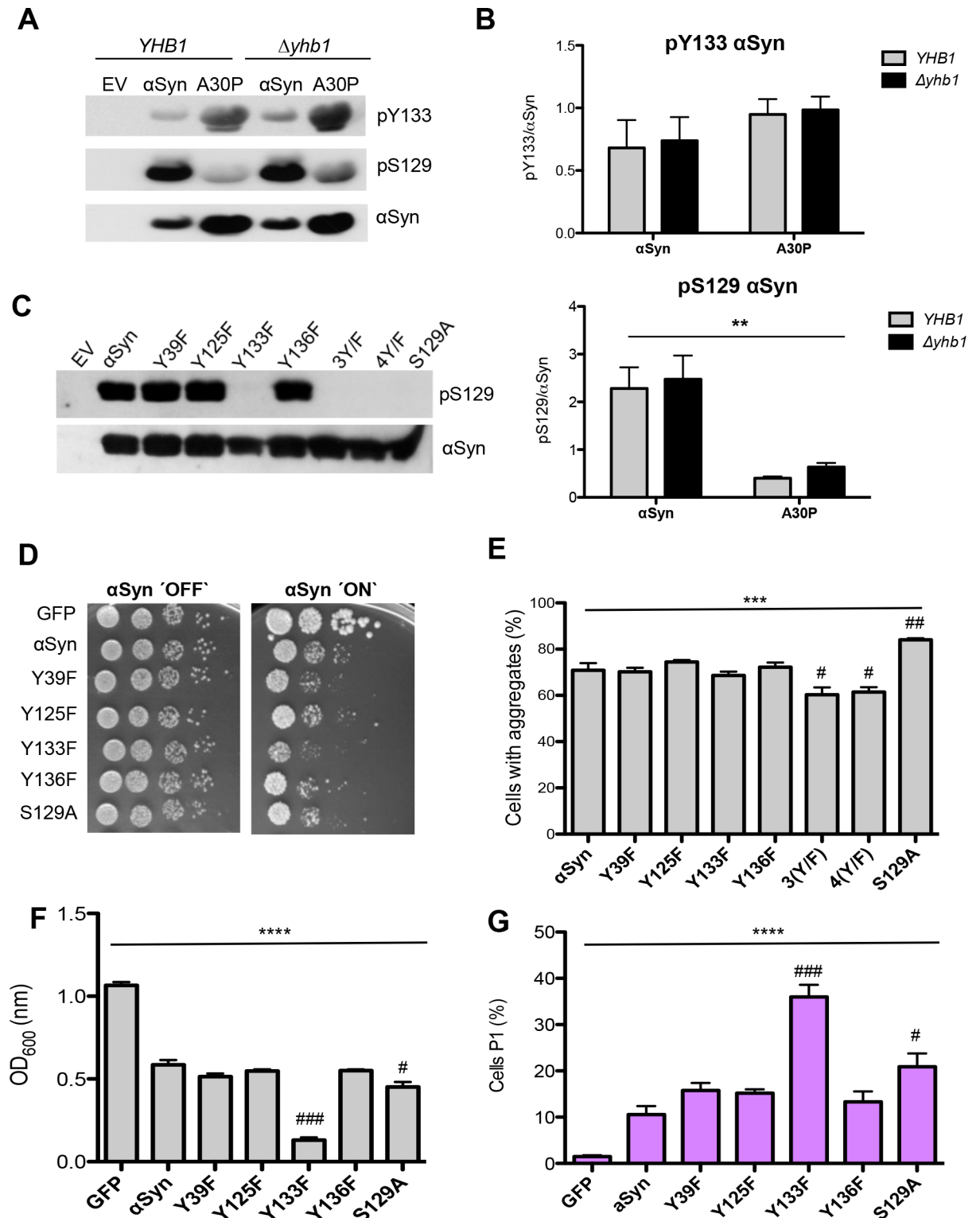


Fig 11. Tyrosine 133 is required for phosphorylation of α Syn at serine 129. (A) Western blotting of α Syn and A30P expressed in YHB1 and $\Delta yhb1$ yeast enriched by Ni²⁺ pull-down, using Y133 phosphorylation-specific α Syn antibody (pY133) and S129 phosphorylation-specific α Syn antibody (pS129). The same membrane was stripped and re-probed with α Syn antibody. (B) Quantification of α Syn and A30P Y133- and S129-phosphorylation levels in YHB1 and $\Delta yhb1$ yeast cells. Densitometric analysis of the immunodetection of pY133, pS129 α Syn and A30P relative to the intensity obtained for α Syn. Significance of differences was calculated with one-way ANOVA test (**, $p < 0.01$; $n = 4$). (C) Western blotting of crude extracts from yeast cells, expressing

different α Syn variants after 6 h induction of protein expression using S129 phosphorylation-specific α Syn antibody (pS129) and α Syn antibody. Cells expressing S129A mutant served as control. (D) Spotting analysis of α Syn and indicated mutant strains, driven by the inducible *GAL1*-promoter on non-inducing ('OFF': glucose) and inducing ('ON': galactose) SC-Ura medium after 3 days. Cells expressing GFP served as control. (E) Quantification of the percentage of cells displaying α Syn aggregates after 6 h induction in galactose-containing SC-Ura medium. Significance of differences was calculated with one-way ANOVA (***, $p < 0.001$) or Dunnett's multiple comparison test (#, $p < 0.05$; ##, $p < 0.01$ versus α Syn; $n = 6$). (F) Cell growth analysis of cells expressing different α Syn variants and GFP (control) after 20 h induction of expression. Significance of differences was calculated with one-way ANOVA (****, $p < 0.0001$) or Dunnett's multiple comparison test (#, $p < 0.05$; ###, $p < 0.001$, $n = 4$). (G) Quantification of cells expressing different α Syn variants and GFP (control) displaying Propidium Iodide (PI) fluorescence after 20 h induction of α Syn expression, assessed by flow cytometry. The percentage of PI-positive yeast cells with higher fluorescent intensities (P1) than the background is presented. Significance of differences was calculated with one-way ANOVA (****, $p < 0.0001$) or Dunnett's multiple comparison test (#, $p < 0.05$; ###, $p < 0.001$ versus α Syn; $n = 4$).

doi:10.1371/journal.pgen.1006098.g011

C-terminal α Syn modifications promote autophagy clearance of α Syn aggregates

GAL1 promoter shut-off experiments were performed to study the role of α Syn PTMs on autophagy/vacuole and proteasome-mediated aggregate clearance of α Syn. The impact of blocking these systems by drug treatments was examined. Expression of α Syn was induced for 4 h in galactose-containing medium and the cells were then shifted to glucose-containing medium in order to repress the promoter. Cells were imaged 4 h after promoter shut-off and the percentage of cells with inclusions was determined. Shut-off studies were performed with wild-type α Syn and the mutants 4(Y/F), S129A and Y133F. PMSF was used as an inhibitor of autophagy/vacuole to study the contribution of this pathway for aggregate clearance [63]. PMSF impairs the activity of many vacuolar serine proteases without affecting proteasome function [84, 85]. Inhibition of autophagy resulted in inefficient aggregate clearance of α Syn, as shown previously [41, 63]. Mutations of the codons for the four tyrosines as well as the S129 and Y133 single exchanges resulted in similar aggregate clearance by inhibition of the autophagic proteases as in the control cells without drug (ethanol) (Fig 13A). This suggests that autophagy is less involved in aggregate clearance of these mutants and shows that autophagy-mediated aggregate clearance requires modifications of the tyrosines and S129. The contribution of the proteasome on 4(Y/F), S129A and Y133F α Syn aggregate clearance was analyzed by applying the proteasome inhibitor MG132 [86]. In contrast to autophagy impairment, cells expressing 4(Y/F) and S129A α Syn cleared inclusions equally as the wild-type α Syn (Fig 13B) when the proteasome system was impaired. These results corroborate our previous findings showing a minor contribution of the proteasome to α Syn aggregate clearance [63]. However, cells expressing the Y133F mutant were unable to clear inclusions in a same manner as the wild-type, 4(Y/F) and S129A α Syn. This indicates that α Syn, which is not modified at Y133, is degraded by the proteasomal pathway. The results suggest that PTMs of tyrosine residues and S129 promote the autophagy-mediated aggregate clearance, whereas non-modified Y133 residue is a key determinant for the targeting of the protein to the proteasome.

Inhibition of autophagy of A30P expressing cells revealed diminished clearance of aggregates of A30P as well as the A30P/4(Y/F) mutant indicating that degradation of the A30P/4(Y/F) aggregates depends on the autophagy/vacuole system similarly to wild-type α Syn and A30P (Fig 13C). A30P/S129A and A30P/Y133F mutants were able to degrade aggregates efficiently upon autophagy inhibition, similar to S129A and Y133F. Proteasome impairment resulted in inefficient clearance of the A30P/Y133F mutant (Fig 13D). However, this impact was not as strong as in the α Syn Y133F mutant, confirming that the wild-type α Syn is strongly dependent on Y133 modification as a determinant for aggregate clearance.

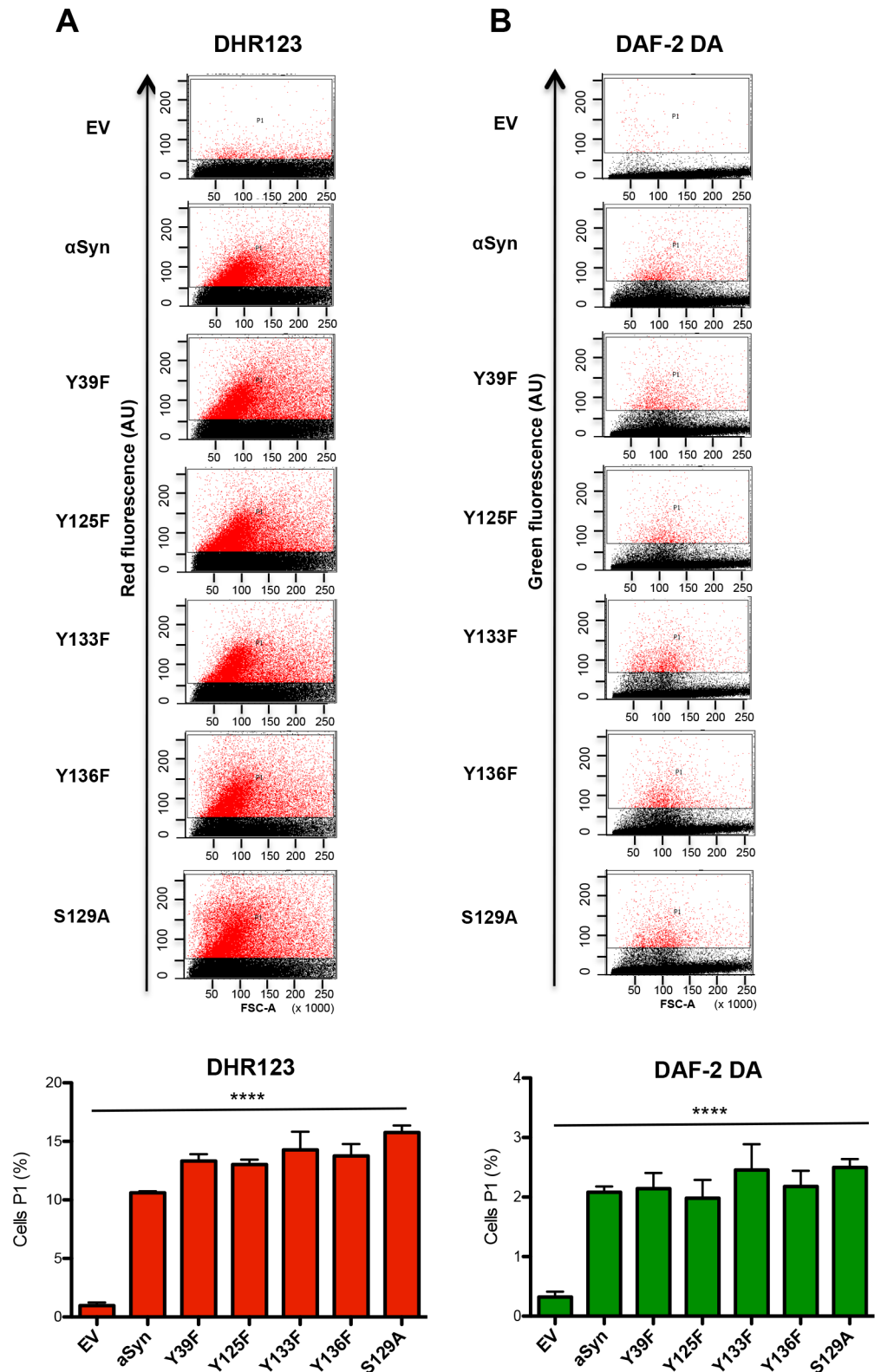


Fig 12. Tyrosine 133 mutation does not alter the accumulation of reactive oxygen and nitrogen species. (A, B) Quantification of cells expressing different α Syn variants displaying ROS and RNS assessed with flow cytometry analysis. α Syn expression was induced for 6 h and the cells were stained for 1.5 h with DHR123 to visualize ROS (A) or with DAF-2 DA to visualize RNS (B). Forward scatter (FSC) and DHR123 (A)

or DAF-2 DA (B) fluorescence of the cells, showing one representative result from at least four independent experiments. The percentage of the sub-populations of yeast cells with higher fluorescent intensities (P1) than the background are presented in the lower panels. Significance of differences was calculated with one-way ANOVA (****, $p < 0.0001$).

doi:10.1371/journal.pgen.1006098.g012

Discussion

Phosphorylation at serine residue S129 represents the major protective phosphorylation site of α Syn which is conserved from man to the baker's yeast as a eukaryotic Morbus Parkinson cell model. The effect of nitrative modifications of α Syn and their contribution towards α Syn-induced cytotoxicity was investigated. A complex interplay was discovered between modifications of the C-terminal tyrosine residues and S129 phosphorylation (Fig 14). These tyrosine

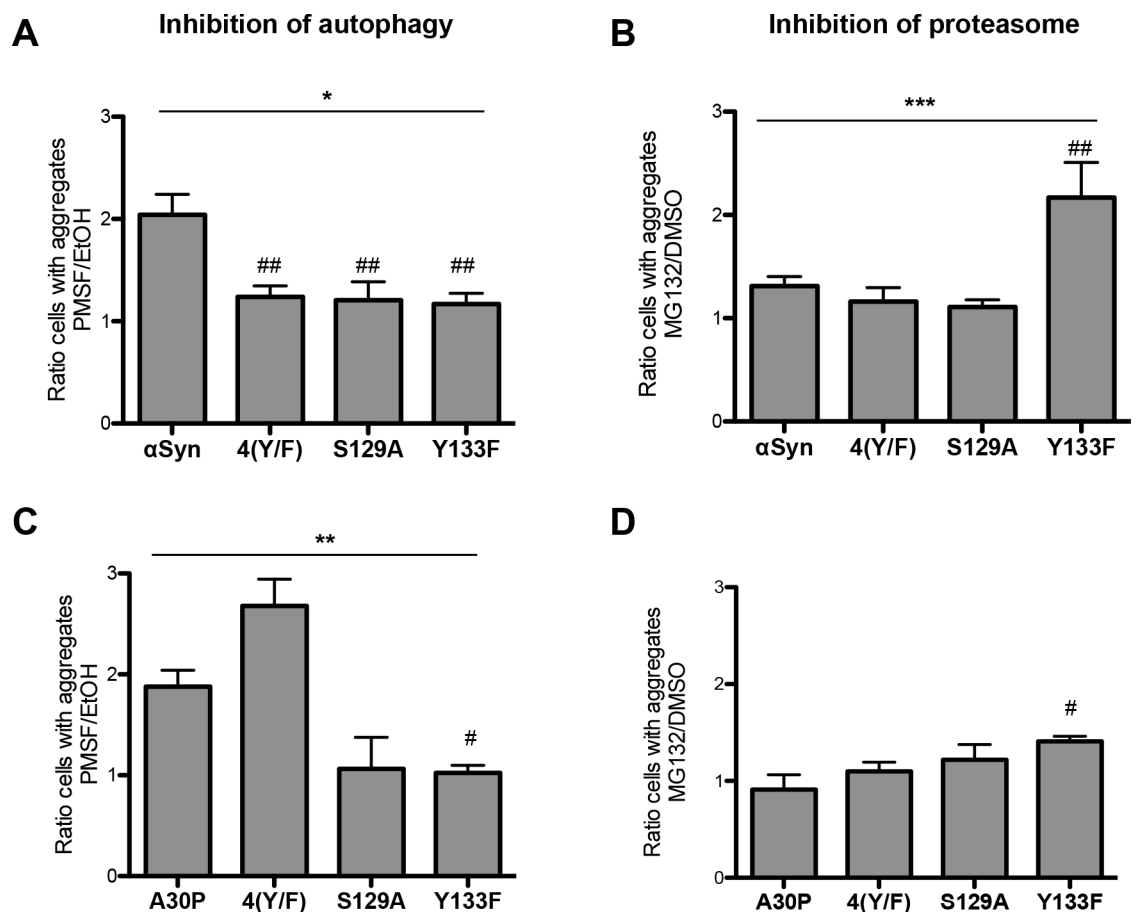


Fig 13. α Syn aggregate clearance after promoter shut-off. (A, C) Quantification of cells displaying aggregates of α Syn (A) and A30P (C) upon inhibition of autophagy by PMSF. Cells expressing α Syn (A) or A30P (C) and its 4(Y/F), S129A and Y133F variants were incubated in 2% galactose-containing media for 4 h and shifted to 2% glucose-containing media supplemented with 1 mM PMSF dissolved in EtOH and only EtOH as a control. Cells with aggregates were counted after 4 h *GAL1*-promoter shut-off and presented as a ratio to the control (EtOH). Significance of differences was calculated with one-way ANOVA (*, $p < 0.05$; **, $p < 0.01$) or Dunnett's multiple comparison test (#, $p < 0.05$; ##, $p < 0.01$ versus α Syn; $n = 4$). (B, D) Quantification of cells displaying aggregates of α Syn (B) and A30P (D) upon inhibition of the proteasome by MG132. Cells expressing α Syn (B) or A30P (D) and the indicated 4(Y/F), S129A and Y133F variants were incubated in 2% galactose-containing media for 4 h and shifted to glucose medium, supplemented with 75 μ M MG132, dissolved in DMSO or only DMSO as a control. Cells with aggregates were counted after 4 h *GAL1*-promoter shut off and presented as a ratio to the control (DMSO). Significance of differences was calculated with one-way ANOVA (***, $p < 0.001$) or Dunnett's multiple comparison test (#, $p < 0.05$; ##, $p < 0.01$ versus α Syn; $n = 4$).

doi:10.1371/journal.pgen.1006098.g013

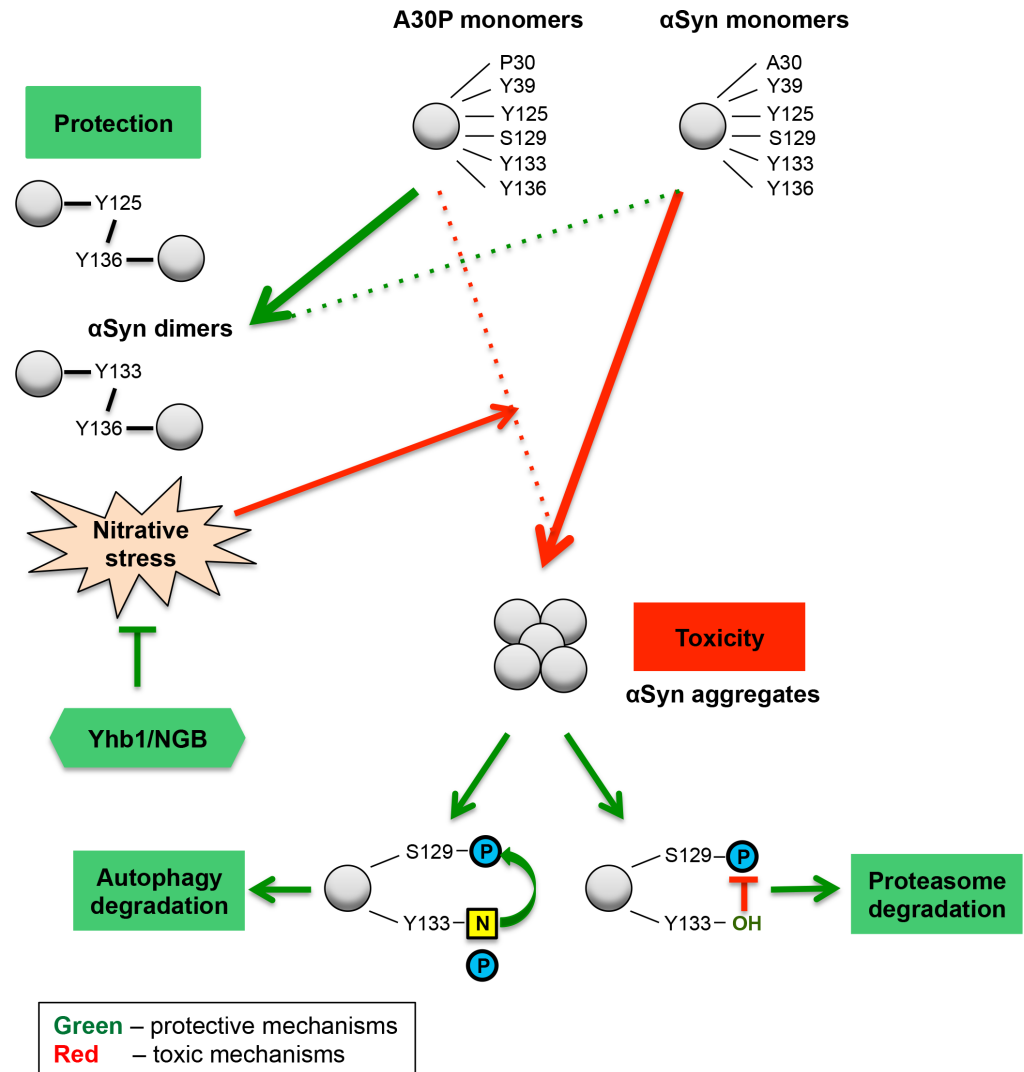


Fig 14. α Syn posttranslational modifications and nitration in yeast. Enhanced intracellular nitrative stress increases the protein nitration level and influences yeast growth and aggregation. The nitration of tyrosine residues acts as trigger for α Syn and A30P toxicity. Wild-type α Syn, which is highly nitrated, inhibits growth and shows a high aggregation rate. A30P is weakly nitrated and therefore, does not inhibit yeast growth and has a low aggregation propensity. Yhb1 and its human homolog NGB protect the cells against accumulation of nitrative species and diminish the aggregate formation. Di-tyrosine crosslinked dimers are formed in reverse correlation to cytotoxicity and do not depend on Yhb1. A30P forms twice as many dimers as the toxic α Syn variant, suggesting that the di-tyrosine crosslinked dimers are not toxic species and are presumably part of a cellular detoxification pathway, sequestering the protein off-pathway of α Syn nucleation. The C-terminal tyrosine modifications have dual effect on the toxicity of the protein. Y133, which is nitrated and phosphorylated, is required for the protective phosphorylation at S129 and for the autophagy degradation of α Syn aggregates. Non-modified Y133 promotes the proteasomal degradation of α Syn aggregates. N: nitration; P: phosphorylation.

doi:10.1371/journal.pgen.1006098.g014

residues of α Syn can be phosphorylated or nitrated with drastic consequences for cellular growth. There is a strong preference of the C-terminus of α Syn for nitration or di-tyrosine formation. Nitration interferes with protective phosphorylation of S129, whereas di-tyrosine formation protects yeast cells. The yeast nitric oxidoreductase Yhb1 as well as its related human protein neuroglobin play protective roles against α Syn aggregation. Yhb1 decreases the nitration level of the A30P variant of α Syn by reducing the accumulation of reactive nitrogen

species, resulting that yeast cells can tolerate increased levels of this α Syn variant without significant growth inhibition.

In yeast, expression of α Syn triggers accumulation of chemically reactive molecules such as ROS and RNS that damage the cell by causing oxidative and nitrative stress which in turn contributes to cell death [66]. Nitration reduces the binding affinity of α Syn to lipid vesicles and therefore disrupts α Syn-membrane interaction [87]. Numerous studies show that oxidative injury of α Syn, specifically nitration of tyrosine residues, contributes directly to the pathology of PD. Nitrative stress was proposed to induce α Syn aggregation as well as α Syn-induced pathology [34, 47, 50, 88–90]. However, also opposing influence of nitrated α Syn has been shown [51, 52]. Thus, the effect of nitrative α Syn modifications and their influence on the toxicity and aggregation of α Syn is still controversial.

In this study, we show that PTMs on α Syn tyrosine residues have a dual impact on α Syn mediated growth inhibition of yeast cells. Previous studies suggested that nitration of α Syn might be responsible for the formation of the proteinaceous inclusions observed in PD brains and for the neuronal loss in the *substantia nigra* [34, 88]. Here, we showed that nitration increases the growth defect induced by α Syn in yeast cells. Tyrosine nitration increases aggregation, mitochondrial fragmentation and growth inhibition. We demonstrated a correlation between the growth impairment, mediated by α Syn and A30P and their nitration level. α Syn, which inhibits yeast growth and has a high aggregation level, is strongly nitrated. In contrast, A30P, which is not toxic to yeast and aggregates to a lesser extent, is weakly nitrated.

Notably, we showed that C-terminal tyrosine 133 is required for the protective phosphorylation of α Syn at S129. α Syn C-terminal tyrosines Y125, Y133 and Y136 are in close proximity to S129, which raises the question whether there is an interplay between different PTMs at these residues. S129-phosphorylated α Syn is abundantly found in Lewy bodies [35, 37]. This phosphorylation site is conserved in yeast and can be used by several endogenous kinases [91]. The effects of S129 phosphorylation are complex and the role of this modification on α Syn-induced toxicity and aggregation is still controversial [38]. In yeast, S129 phosphorylation has a protective role against growth impairment and aggregate formation [39–41]. Phosphorylation of the tyrosine residues of α Syn is less explored and the effects of this modification are still unclear, varying from protective to no impact on neurotoxicity and oligomerization [83, 92–97]. We show for the first time that tyrosine 133 is strictly required for phosphorylation at S129 in yeast. Tyrosine 133 can be nitrated or phosphorylated, as demonstrated by immunoblotting and MS analysis. These two PTMs might have opposing roles on the cellular toxicity of the protein. Phosphorylation might prevent tyrosine residues from nitration and *vice versa*. Here, we used tyrosine to phenylalanine exchanges that abolishes both phosphorylation as well as nitration. There are no natural amino acids that mimic the phosphorylation or nitration state of the tyrosine residue, thus restricting the investigation of the contribution of a single posttranslational modification at one and the same tyrosine residue *in vivo*. Our results reveal Y133 as major tyrosine phosphorylation site in yeast, and we observe only insignificant phosphorylation at Y125. Our data reveal a correlation between tyrosine nitration and the cellular S129 phosphorylation level. The wild-type α Syn has significantly higher nitration levels as well as increased protein populations with S129 phosphorylation but similar levels of Y133 phosphorylation when compared to its A30P variant. These results suggest that rather nitration than phosphorylation at Y133 promotes S129 phosphorylation in yeast. Alternatively, nitration at Y133 might change the protein conformation and make S129 more accessible for protein kinases. The protective effect of Y133 was not accompanied with changes in the potential to form aggregates. The discrepancy between the clear protective effect of Y133 on yeast growth without significant effect on inclusion formation suggests that additional yet elusive protective mechanisms exist in the cell, which do not depend on aggregate formation but support cellular

survival. This suggests an even more complicated interplay between different α -synuclein modifications. Recently, the role of site-specific nitration of α Syn was investigated using site-specifically nitrated synthetic proteins at Y39 and Y125 [98]. The authors assessed the influence of nitration at Y125 and Y39 on PLK3-mediated *in vitro* phosphorylation at S129 and showed that tyrosine nitration does not prevent recognition of the protein by PLK3 and the subsequent phosphorylation at S129. These results strengthen the link between the C-terminal tyrosine and serine modifications, revealing a complex cross-talk between PTMs with different contributions to the cytotoxicity of α Syn.

Previously, we have shown that autophagy is the major pathway for aggregate clearance in yeast [63]. The phosphorylation state of α Syn influences the clearance mechanism of the protein. Blocking of S129 phosphorylation in yeast leads to impaired aggregate clearance by autophagy [39]. Increased levels of S129 phosphorylation can suppress the defect of impaired α Syn sumoylation by rescuing the autophagic aggregate clearance and promoting the proteasomal clearance of α Syn [41]. Here, we show that posttranslational modifications of the four tyrosine residues, similar to S129 phosphorylation, promote the autophagic clearance of α Syn aggregates. Inhibition of autophagy rendered yeast cells unable to clear α Syn aggregates, however had no effect on the clearance of S129A, 4(Y/F) and Y133F mutants. Interestingly, Y133F mutant could not be degraded upon inhibition of the proteasome. Similarly, proteasome impairment resulted in inefficient clearance of the A30P/Y133F mutant, however the impact was not as strong as in the α Syn Y133F mutant. Therefore, Y133 represents a key determinant for the degradation fate of α Syn. Phospho- and nitro-modifications at Y133 promote the autophagic clearance of the aggregates, whereas the non-modified Y133 protein is directed to the proteasome.

Beside nitration, the reaction between tyrosine and RNS can result in the formation of di-tyrosine bonds, leading to the formation of stable α Syn oligomers, including dimers and higher oligomeric structures. At low peroxynitrite level, di-tyrosine formation outcompetes the reaction of tyrosine nitration [54, 55] indicating a forced reaction to tyrosine nitration under nitrative stress. We observed formation of dimers and oligomers *in vivo* without exposure of yeast cells to nitrating agents; therefore, they represent the consequence of endogenous nitrative stress. Previous studies already demonstrated nitration-induced oligomerization of α Syn [42, 53]. There, treatment with nitrating agent resulted in the formation of α Syn dimers and oligomers crosslinked by di-tyrosine bonds. Using MS, we characterized the tyrosine residues involved in covalent dimer formation and nitration and identified to what extent the different tyrosine residues are involved in the di-tyrosine formation and what are the precise positions of the respective tyrosines. To the best of our knowledge, this is the first characterization of α Syn dimer species, formed *in vivo* and without additional exposure to nitrative agents. Our data reveal strong preference of the C-terminal tyrosine residues for dimer formation with predominant forms including Y136 interacting either with Y125 (Y125-Y136) or with Y133 (Y133-136). Y39 was hardly involved in dimer formation under physiological conditions in yeast or *in vitro* after PON treatment. Recently, *in vitro* studies on α Syn oligomerization and di-tyrosine formation upon treatment with tetranitromethane (TMN) demonstrate a predominant formation of di-tyrosine dimers when Y39 is not available for nitration (Y39F) and suggest that the N-terminal region of α Syn plays a role in TMN-induced di-tyrosine formation of higher order oligomers [98].

There are studies which described an increase of nitration at Y39 of α Syn in an oxidative cellular model of PD [99], whereas we observe resistance of Y39 to 3-NT modification in comparison to the C-terminal tyrosine residues which are nitrated *in vitro* as well as *in vivo*. These results are corroborated by previous findings, where treatment of purified α Syn with PON did not result in nitration of Y39; however, all C-terminal residues were nitrated [100]. Higher nitration levels of α Syn compared to A30P were also detected by mass spectrometry data

confirming the results from western blot analyses. There, only one tyrosine residue is nitrated in A30P, whereas three α Syn residues are nitrated.

Our data reveal that α Syn dimers originating from di-tyrosine crosslinking are non-toxic species in contrast to nitrated α Syn. Covalent binding of the di-tyrosines stabilizes the dimeric structures and consequently removes α Syn molecules from aggregation to toxic aggregates. α Syn protein lacking all four tyrosine residues forms less aggregates, however, the aggregate formation is not prevented. This indicates that tyrosine residues are not crucial for *in vivo* assembly of the protein to aggregates and suggests an independent pathogenic mechanism of α Syn aggregation. Similarly, nitration of α Syn was shown to promote formation of stable off-pathway oligomeric species that inhibit α Syn fibrillation [51, 52]. Thus, the formation of stable oligomers under oxidative stress conditions redirects the monomers to oligomers that do not contribute to fibril formation.

Expression of A30P in yeast has different toxicity properties from wild-type α Syn [60, 63]. A30P is located in the cytoplasm, whereas α Syn is delivered to the plasma membrane. Overexpression from a high-copy number plasmid results in formation of A30P fluorescent foci, however, the aggregation is transient and yeast cell growth is not affected. Using the $\Delta yhb1$ mutant lacking the flavohemoglobin Yhb1, we could demonstrate that nitration plays also a role for A30P and confirmed that nitration increases aggregation and growth inhibition. Deletion of the *yhb1* yeast gene results in a deficient cellular detoxification machinery towards NO and makes A30P as toxic as wild-type α Syn. This shows that the A30P nitration level is a crucial factor for gaining toxicity. Consequently, elimination of its putative NO-detoxifier Yhb1 results in stronger formation of toxic α Syn aggregates. Yhb1 reduced the level of nitrative stress in A30P expressing cells. Moreover, Yhb1 protected the A30P-expressing cells from mitochondrial fragmentation. α Syn-induced fragmentation of mitochondrial structure caused by direct interaction of α Syn with the mitochondrial membranes was already demonstrated [78]. It was proposed that ROS accumulation induced by α Syn expression is an indirect effect due to mitochondrial dysfunction [65]. We found a connection between increased nitrative stress and mitochondrial fragmentation. This suggests a mechanistic model based on the specific ability of α Syn and A30P to form aggregates and damage mitochondria induced by nitrative stress.

Analysis of neuroglobin (NGB), the human homologue of *YHB1*, in human cell lines (H4 cells) confirmed that this protein modulates α Syn aggregation. Expression of neuroglobin in mammalian cells reduced the number inclusions per cell. Neuroglobin is expressed primarily in neurons and protects against hypoxic neuronal death and ischemic brain injury [101]. Furthermore, expression of neuroglobin protects against beta-amyloid-induced neurotoxicity in transgenic mice *in vivo* [80]. Recent reports revealed that overexpression of neuroglobin prevents tau hyperphosphorylation at multiple AD-related sites [102]. These data support our findings and imply NGB as a new therapeutic target in PD and other neurodegenerative diseases.

A complex interplay between nitration and phosphorylation of α Syn C-terminal residues, deeply interconnected with nitrative stress, determines the aggregate clearance by autophagy or ubiquitin-dependent 26S proteasome pathways (Fig 14). The proposed model derived from yeast as unicellular eukaryotic cell should provide interesting hints and insights for the study of α Syn posttranslational communications as it happens in the human brain and its connection to oligomer or aggregate formation and clearance.

Materials and Methods

Plasmid construction, yeast strains, transformation and growth conditions

Plasmids (Table 2) and *Saccharomyces cerevisiae* strains (Table 3) used in this work are listed below. Human α Syn cDNA sequence and the corresponding A30P sequence were expressed

Table 2. Plasmids used in this study.

Plasmid	Description	Source
pME2788	<i>pRS413-GAL1-promoter, CYC1-terminator, HIS3, CEN/ARS, pUC origin, Amp^R</i>	[104]
pME2795	<i>pRS426-GAL1-promoter, CYC1-terminator, URA3, 2μm, pUC origin, Amp^R</i>	[104]
pME3759	pME2795 with <i>GAL1::GFP</i>	[63]
pME3760	pME2795 with <i>GAL1::SNCA^{WT}</i>	[63]
pME3761	pME2795 with <i>GAL1::SNCA^{A30P}</i>	[63]
pME3763	pME2795 with <i>GAL1::SNCA^{WT}::GFP</i>	[63]
pME3764	pME2795 with <i>GAL1::SNCA^{A30P}::GFP</i>	[63]
pME4095	pME2795 with <i>GAL1::SNCA^{WT}::6 x HIS</i>	[41]
pME4101	pME2795 with <i>GAL1::SNCA^{A30P}::6 x HIS</i>	This study
pME4104	pME2788 with <i>GAL1::NGB</i>	This study
pME4351	pME2788 with <i>GAL1::YHB1</i>	This study
pME4352	pME2795 with <i>GAL1::SNCA^{WT}Y39/125/133/136F::GFP</i>	This study
pME4353	pME2795 with <i>GAL1::SNCA^{WT}Y39/125/133/136F::6 x HIS</i>	This study
pME4354	pME2795 with <i>GAL1::SNCA^{A30P}Y39/125/133/136F::6 x HIS</i>	This study
pME4355	pME2795 with <i>GAL1::SNCA^{A30P}Y39/125/133/136F::GFP</i>	This study
pcDNA3.1		Invitrogen
pME4357	pcDNA3.1 with <i>CMV::NGB::mCherry</i>	This study
pME4088	pME2795 with <i>GAL1::SNCA^{WT}Y125F::GFP</i>	This study
pME4451	pME2795 with <i>GAL1::SNCA^{WT}Y39F::GFP</i>	This study
pME4452	pME2795 with <i>GAL1::SNCA^{WT}Y39F::6 x HIS</i>	This study
pME4453	pME2795 with <i>GAL1::SNCA^{WT}Y125F::6 x HIS</i>	This study
pME4454	pME2795 with <i>GAL1::SNCA^{WT}Y125/133/136F::GFP</i>	This study
pME4455	pME2795 with <i>GAL1::SNCA^{WT}Y125/133/136F::6 x HIS</i>	This study
pME4456	pME2795 with <i>GAL1::SNCA^{WT}S129A::GFP</i>	This study
pME4457	pME2795 with <i>GAL1::SNCA^{WT}S129A::6 x HIS</i>	This study
pME4460	pME2795 with <i>GAL1::SNCA^{WT}Y133F::6 x HIS</i>	This study
pME4461	pME2795 with <i>GAL1::SNCA^{WT}Y133F::GFP</i>	This study
pME4462	pME2795 with <i>GAL1::SNCA^{WT}Y136F::6 x HIS</i>	This study
pME4463	pME2795 with <i>GAL1::SNCA^{WT}Y136F::GFP</i>	This study
pME4466	pME2795 with <i>GAL1::SNCA^{A30P}S129A::GFP</i>	This study
pME4467	pME2795 with <i>GAL1::SNCA^{A30P}Y133F::GFP</i>	This study

doi:10.1371/journal.pgen.1006098.t002

from yeast high expression vector (2 μ) under the *GAL1* promoter and *CYC1* terminator as described previously [63]. *YHB1* sequence was amplified on genomic DNA from *Saccharomyces cerevisiae* and *NGB* was amplified on cDNA sequence and cloned into pME2788 low copy vector (*CEN/ARS*) preceded by *GAL1* promoter and followed by *CYC1* terminator, respectively. The 4(Y/F) α Syn mutant constructs were generated by site-directed mutagenesis using QuickChange II Site-Directed Mutagenesis Kit (Agilent Technologies). Plasmids pME3763, pME3764, pME4095 and pME4101 were used as templates to substitute the four tyrosines (Y39, Y125, Y133, Y136) by phenylalanine. The same plasmids were used as templates to

Table 3. Yeast strains used in this study.

Strain	Genotype	Source
BY4741	<i>MATa; his3Δ 1; leu2Δ0; met15Δ0; ura3Δ0</i>	EUROSCARF
Δ yhb1	<i>BY4741; MATa; his3Δ1; leu2Δ0; met15Δ0; ura3Δ0; YGR234w::kanMX4</i>	EUROSCARF

doi:10.1371/journal.pgen.1006098.t003

substitute serine 129 by alanine. For growth and microscopy studies, α Syn variants were used that are C-terminally tagged with GFP via the KLID linker [63]. For Ni²⁺-NTA affinity chromatography, α Syn and A30P were C-terminally fused to His₆-tag using pME3760 and pME3761 as templates. All constructs were verified by DNA sequencing.

Saccharomyces cerevisiae strains, BY4741 and $\Delta yhb1$, were grown in non-selective medium (YEPD) at 30°C and transformed by standard lithium acetate protocol [103]. For cultivation of the $\Delta yhb1$ strain, 200 μ g/ml G418 were added to the medium. Transformants harboring α Syn constructs were selected on solid Synthetic Complete medium (SC) lacking uracil (SC-Ura) supplemented with 2% glucose for 2 days at 30°C. For growth of cells co-expressing α Syn with *YHB1* and *NGB*, respectively, SC medium lacking uracil and histidine (SC-Ura-His) was used. Expression of α Syn was induced by shifting overnight cultures from 2% raffinose- to 2% galactose-containing medium ($A_{600} = 0.1$).

Spotting assay and growth analysis in liquid culture

To investigate growth on solid medium, cells were pre-grown in selective SC medium containing 2% raffinose. After normalizing the cells to equal densities ($A_{600} = 0.1$), 10-fold dilution series were prepared and spotted in a volume of 10 μ l on SC-Ura or SC-Ura,-His agar plates supplemented with either 2% glucose or 2% galactose. The growth was documented after incubation for 3 days at 30°C. For growth test in liquid cultures, cell cultures were pre-grown as described above, adjusted to equal densities of $A_{600} = 0.1$ and shifted to galactose-containing SC-Ura medium. Optical density measurements of 200 μ l cell cultures were performed in 96-well plates for 48 h using a microplate reader (Infinite M200; TECAN Group Ltd). Growth analyses under nitrative stress conditions were performed using either 600 μ M or 1 mM DETA-NONOate (Cayman Chemical Company) as NO donor in SC-Ura medium at pH 7.4.

Fluorescence microscopy, mitochondrial staining and quantifications

Cells were pre-grown in selective SC medium containing raffinose and inoculated in galactose-containing SC medium to an $A_{600} = 0.1$. α Syn expression was induced for 6 h and fluorescent images were obtained with 63x magnification using a Zeiss Observer. Z1 microscope (Zeiss) equipped with a CSU-X1 A1 confocal scanner unit (YOKOGAWA), QuantEM:512SC digital camera (Photometrics) and SlideBook 6.0 software package (Intelligent Imaging Innovations). Depending on the fluorescent agent, ssGFP or sdRFP filter were applied. To quantify aggregation, at least 300 cells were counted per strain and experiment and the number of cells displaying α Syn aggregation was referred to the total number of counted cells. To label mitochondria, the cells were incubated for 45 minutes (min) in the presence of 50 nM Mito-Tracker Red (Molecular Probes, Invitrogen), washed once with fresh medium and imaged. To test yeast for production of ROS, cells pre-grown overnight in raffinose-containing SC medium were transferred to galactose-containing SC medium at $A_{600} = 0.1$ and incubated for 6 h at 30°C. After washing the cells, dihydrorhodamine 123 (DHR123) (Cayman Chemical Company) was added to a final concentration of 5 μ g/ml and the cells were incubated for 1.5 h at 30°C. After washing, the cells were re-suspended in H₂O and microscopy was performed using RFP filter. To test yeast for RNS production, cells pre-grown overnight in raffinose-containing SC medium were transferred to galactose-containing SC medium at $A_{600} = 0.1$. After 6 h induction cells were washed and diluted in PBS buffer, pH 7.5 to $A_{600} = 0.1$. DAF-2 DA (Genaxxon bioscience GmbH) was added to a final concentration of 25 μ g/ml and cells were incubated for 1 h at 30°C in the dark. Before microscopy, the cells were washed and RNS was visualized using GFP filter.

Flow cytometry

For testing yeast cells for production of ROS and RNS, flow cytometry was performed. Cells were grown as above. Before measuring, cells were re-suspended in 50 mM trisodium citrate buffer, pH 7.0. Flow cytometry analysis was performed on a BD FACSCANTO II (Becton Dickinson). 100 000 events were counted for each experiment. Data analysis was performed using the BD FACSDIVA software (Becton Dickinson). Representative examples that are shown in the Figures were repeated at least 3 times. Yeast cell membrane integrity was analyzed with PI staining. Yeast cells were incubated with 12.5 μ g/ml PI for 30 min. As a positive control, cells were boiled for 10 min at 95°C.

Promoter shut-off assay and chemical treatments

Yeast cells carrying α Syn were pre-grown in selective SC medium containing 2% raffinose overnight and shifted to 2% galactose-containing selective SC medium to induce the α Syn expression for 4 h. Afterwards, cells were shifted to SC medium supplemented with 2% glucose to shut-off the promoter. 4 h after promoter shut-off, cells were visualized by fluorescence microscopy. The reduction of number of cells displaying α Syn inclusions was recorded and plotted on a graph. To study the lysosome/vacuole degradation pathway (autophagy) phenylmethanesulfonyl fluoride (PMSF) in ethanol (EtOH) was applied to the suspension in a final concentration of 1 mM [105]. For impairment of the proteasomal degradation system Carbo-benzoxyl-leucinylleucinyl-leucinal (MG132) dissolved in dimethyl sulfoxide (DMSO) was added to the cell suspension in a final concentration of 75 μ M and in parallel, equal volume of DMSO was applied to the cells as a control. For drug treatment with MG132 induction-medium containing galactose and shut-off-medium containing glucose was supplemented with 0.003% SDS and 0.1% proline [106].

Ni²⁺-NTA affinity chromatography and *In vitro* nitration

Purification of His₆-tagged recombinant α Syn and A30P was performed using yeast cells carrying the 2 μ high-copy vectors pME4095 and pME4101, pME4353, pME4354 and pME2795. Cells cultured overnight in 200 ml selective SC medium supplemented with 2% glucose were collected by centrifugation, washed and inoculated in 1.5 liter selective medium containing 2% galactose for 12 h at 30°C. Cells were lysed by 50 ml 1.85 M NaOH containing 7.5% β -mercaptoethanol on ice for 10 min. For precipitation, the protein crude extracts were incubated for 30 min in 50 ml 50% trichloroacetic acid (TCA) on ice, washed afterwards with acetone and dissolved in 50 ml buffer A (6 M Guanidine hydrochloride, 100 mM NaH₂PO₄, 10 mM Tris-HCl, pH 8.0). The mixture was shaken for 1 h at 25°C, the collected supernatant was calibrated to pH 7.0 with 1 M Tris base (pH 8.5) and supplemented with imidazole to final concentration of 20 mM. Before the protein crude extract was applied to a His GraviTrap column (GE Healthcare Life Science), the columns were washed with 10 ml buffer A containing 20 mM imidazole and equilibrated with 5 ml buffer B (8 M Urea, 100 mM Na₃PO₄, 10 mM Tris, pH 6.3). Elution of the protein was carried out using 4 times 1 ml of 200 mM imidazole resolved in buffer B. The protein content of the elution fractions were determined by Bradford protein concentration assay and subjected to western blot analysis. *In vitro* nitration of α Syn was performed using the highly reactive nitrating agent peroxyxynitrite (PON) (Cayman Chemical Company) in the presence of 0.3 M HCl to adjust the pH value. 20 μ l of the protein were mixed with 1 μ l of both reagents for approximately 10 seconds.

Immunoblotting

Yeast cells harboring different α Syn constructs were grown in selective SC medium containing 2% raffinose overnight and transferred to 2% galactose-containing medium for induction of α Syn expression. After expression of α Syn for 6 h, protein crude extracts were prepared and protein concentration was determined via Bradford protein concentration assay. For electrophoretic separations of the protein, 10 μ g protein extract was applied to a 12% SDS-polyacrylamide-gel and transferred afterwards onto a nitrocellulose or polyvinylidene difluoride (PVDF) membrane. The membrane was incubated with primary antibody diluted in TBST buffer with 5% milk powder overnight. As primary antibodies, rabbit anti $\alpha/\beta/\gamma$ Syn polyclonal antibody (1:2000, Santa Cruz Biotechnology), mouse anti 3-nitrotyrosine monoclonal (1:1400, Abcam), mouse anti nitro- α/β Syn (Tyr39) monoclonal antibody (1:2000, MERCK), mouse anti di-tyrosine monoclonal antibody (1:1000, JaICA), mouse anti phospho Ser-129 α Syn antibody (1:2500, Wako Chemicals USA), rabbit anti phospho Tyr-133 α Syn polyclonal antibody (1:1000, Abcam) and mouse anti GAPDH monoclonal antibody (1:5000, Thermo Fisher Scientific) were used. Peroxidase-coupled goat anti mouse (1:2000, Jackson ImmunoResearch Laboratories) or goat anti rabbit (1:5000, Mobitec) immunoglobulins G was applied as secondary antibody.

Quantifications of Western Blots

Pixel density values for Western Blot quantification were obtained from TIFF files generated from digitized x-ray films (Kodak) and analyzed with the ImageJ software (NIH, Bethesda). Sample density values were normalized to the corresponding loading control. For quantification of the signals, at least three independent experiments were performed. The significance of differences was calculated using Student's t test or one-way ANOVA test. p value < 0.05 was considered to indicate a significant difference.

Mass spectrometry analysis

Protein samples were separated by 12% SDS-PAGE. Excised polyacrylamide gel slices of Coomassie stained proteins were digested with the proteases trypsin (Promega) and AspN (Sigma-Aldrich) according to the protocol of Shevchenko [107] and supplier's instructions. After digestion and peptide elution the samples were resolved in 20 μ l 2.8% acetonitrile containing 0.1% formic acid. The single digestions as well as the double digested AspN/tryptic peptides were then analyzed by LC-MS.

Peptides of 1–5 μ l sample solution were trapped and washed with 0.07% trifluoroacetic acid 2.6% acetonitrile on an Acclaim PepMap 100 column (100 μ m x 2 cm, C18, 3 μ m, 100 \AA , P/N164535 Thermo Scientific) at a flow rate of 25 μ l/min for 5 min. Analytical peptide separation by reverse phase chromatography was performed on an Acclaim PepMap RSLC column (75 μ m x 25 cm, C18, 3 μ m, 100 \AA , P/N164534 Thermo Scientific) running a 40 min gradient from 100% solvent A (0.1% formic acid) to 65% solvent B (80% acetonitrile, 0.1% formic acid) and further to 95% solvent B within 1 min at flow rates of 300 nl/min (Fisher Chemicals). Chromatographically eluting peptides were on-line ionized by nano-electrospray (nESI) using the Nanospray Flex Ion Source (Thermo Scientific) at 2.4 kV and continuously transferred into the mass spectrometer. Full scans within m/z of 300–1850 were recorded with the Orbitrap-FT analyzer at a resolution of 30,000 with parallel data-dependent top 10 MS²-fragmentation in the LTQ Veleo Pro linear ion trap. LC-MS method programming and data acquisition was performed with the software Xcalibur 2.2 (Thermo Fisher). MS/MS² data processing for protein analysis and PTM identification was done with the Proteome Discoverer 1.4 (PD, Thermo Scientific) software using the SequestHT search engine (Thermo Scientific) and *Saccharomyces*

cerevisiae protein database extended by the most common contaminants with the following criteria: peptide mass tolerance 10 ppm, MS/MS ion mass tolerance 0.8 Da, and up to two missed cleavages allowed. Only high confident peptides with a false discovery rate less than 0.01 were considered.

Identification of crosslinked peptides

The MS data of crosslinked peptides were analyzed with StavroX2.3.4.5 [73]. MS data in the Mascot generic file (mgf) format containing all MS/MS data of precursor ions were loaded into the program. The following parameters were used for the StavroX analysis: (i) cleavage sites: C-terminal: K, R; N-terminal: D; (ii) number of missed cleavages = 2; (iii) variable modifications: oxidation of methionine; nitration of tyrosine; cysteine-to-cysteine acetamid; (iv) mass of crosslinker: -H₂; (v) crosslinks only between two tyrosines; (vi) precision precursor comparison = 10 ppm.

The false-positive rate was evaluated by decoy analysis using the reversed protein sequence. The frequency of occurrence of candidates from the data analysis and decoy analysis was compared for each sample. Only scores with decoy frequencies below 8% of the data frequency were considered as possible crosslinks. The data were filtered for unique scans and each scan was considered only once with its highest score. Since multiple tyrosine residues are located on one and the same peptide, different combinations of crosslinked peptides with equal masses were possible. For each scan the crosslinked tyrosine dimers were assigned according to the score calculated by the program based on the fragment ions series.

Cell culture

Neuroglioma (H4) cells were plated 24 h prior to transfection, in 12-well plates (Costar). Cells were transfected with FuGENE6 Transfection Reagent (Promega) using equal amounts of plasmid DNA encoding for α Syn, synphilin-1 [108] and Neuroglobin-mCherry, or the empty mammalian expression vector pcDNA 3.1, according to the manufacturer's instructions.

Immunocytochemistry

48 h after transfection, cells were washed with PBS and fixed with 4% paraformaldehyde for 10 min at room temperature (RT). After washing with PBS, cells were permeabilized with 0.5% Triton X-100/PBS (Sigma-Aldrich) for 20 min at RT, and blocked in 1.5% normal goat serum (PAA)/PBS for 1 h. Cells were incubated with a mouse anti α Syn antibody (1:1000, BD Transduction Laboratory) overnight and then with a secondary antibody (Alexa Fluor 488 donkey anti-mouse IgG) for 2 h at RT. Finally, cells were stained with Hoechst 33258 (1:5000 in PBS, Life Technologies- Invitrogen) for 5 min and maintained in PBS prior to epifluorescence microscopy.

Quantification of α Syn inclusions and cytotoxicity test in H4 cells

Transfected cells were scored based on the α Syn inclusions pattern and classified into: cells without inclusions, less than ten inclusions (<10 inclusions), and more than ten inclusions (\geq 10 inclusions), as described [61]. The total number of transfected cells was expressed in percentage, as the average from three independent experiments. The lactate dehydrogenase (LDH) cytotoxicity assay (Roche Diagnostics) was performed according to the manufacturer's instructions. Growth media from cells were applied in triplicates in a 96-well plate, in a ratio 1:1 with the reaction mixture. The measurements were performed in a TECAN Infinite 200 Pro plate reader at 490 nm. The percentage of toxicity was calculated as indicated by the manufacturer.

Statistical analysis

Data were analyzed using GraphPad Prism 5 (San Diego, California, USA) Software and were presented as mean \pm SEM of at least three independent experiments. The significance of differences was calculated using Students t-test, one-way ANOVA test with Bonferroni's multiple comparison test or Dunnett's multiple comparison test. P value < 0.05 was considered to indicate a significant difference.

Supporting Information

S1 Fig. MS2 analysis of cross-linked peptides. (A) Exemplary fragment ion MS2 spectrum of the crosslink between Y133 and Y136 for α Syn dimers. y -ions of the crosslinked peptides are represented in blue, while b -ions are represented in red. Fragmentation sites are indicated in the amino acid sequence. (B) Exemplary fragment ion MS2 spectrum of the crosslink between Y125 and Y136 of A30P dimers.

(PDF)

S2 Fig. Forward scatter (FSC) and Propidium Iodide (PI) fluorescence intensity of cells assessed with flow cytometry analysis. Cells expressing different α Syn variants and GFP (control) after 20 h induction of expression were stained with 12.5 μ g/ml PI for 30 min. Shown is one representative result from at least four independent experiments.

(PDF)

Acknowledgments

We thank Maria Meyer for excellent technical assistance. We thank Lara Schmitz, Maria Kuzyakova and Alexander Hempelmann for help with the experimental work.

Author Contributions

Conceived and designed the experiments: AK BP TFO GHB. Performed the experiments: AK BP DFL RP. Analyzed the data: AK BP DFL TFO GHB. Contributed reagents/materials/analysis tools: OV TFO. Wrote the paper: AK BP GHB.

References

1. de Rijk MC, Launer LJ, Berger K, Breteler MM, Dartigues JF, Baldereschi M, et al. Prevalence of Parkinson's disease in Europe: A collaborative study of population-based cohorts. Neurologic Diseases in the Elderly Research Group. *Neurology*. 2000; 54(11 Suppl 5):S21–3.
2. German DC, Manaye K, Smith WK, Woodward DJ, Saper CB. Midbrain dopaminergic cell loss in Parkinson's disease: computer visualization. *Ann Neurol*. 1989; 26(4):507–14. PMID: [2817827](#)
3. German DC, Manaye KF, Sonsalla PK, Brooks BA. Midbrain dopaminergic cell loss in Parkinson's disease and MPTP-induced parkinsonism: sparing of calbindin-D28k-containing cells. *Ann N Y Acad Sci*. 1992; 648:42–62. PMID: [1353337](#)
4. Gibb WR, Lees AJ. Anatomy, pigmentation, ventral and dorsal subpopulations of the substantia nigra, and differential cell death in Parkinson's disease. *Journal of neurology, neurosurgery, and psychiatry*. 1991; 54(5):388–96. Epub 1991/05/01. PMID: [1865199](#)
5. Fedorow H, Tribi F, Halliday G, Gerlach M, Riederer P, Double KL. Neuromelanin in human dopamine neurons: comparison with peripheral melanins and relevance to Parkinson's disease. *Progress in neurobiology*. 2005; 75(2):109–24. Epub 2005/03/24. PMID: [15784302](#)
6. Bellucci A, Mercuri NB, Venneri A, Faustini G, Longhena F, Pizzi M, et al. Review: Parkinson's disease: from synaptic loss to connectome dysfunction. *Neuropathology and applied neurobiology*. 2016; 42(1):77–94. Epub 2015/11/28. doi: [10.1111/nan.12297](#) PMID: [26613567](#)
7. Sung VW, Nicholas AP. Nonmotor symptoms in Parkinson's disease: expanding the view of Parkinson's disease beyond a pure motor, pure dopaminergic problem. *Neurologic clinics*. 2013; 31(3 Suppl):S1–16. Epub 2013/08/16. doi: [10.1016/j.ncl.2013.04.013](#) PMID: [23931951](#)

8. Chaudhuri KR, Healy DG, Schapira AH. Non-motor symptoms of Parkinson's disease: diagnosis and management. *The Lancet Neurology*. 2006; 5(3):235–45. Epub 2006/02/21. PMID: [16488379](#)
9. Spillantini MG, Schmidt ML, Lee VM, Trojanowski JQ, Jakes R, Goedert M. Alpha-synuclein in Lewy bodies. *Nature*. 1997; 388(6645):839–40. PMID: [9278044](#)
10. Spillantini MG, Crowther RA, Jakes R, Hasegawa M, Goedert M. alpha-Synuclein in filamentous inclusions of Lewy bodies from Parkinson's disease and dementia with lewy bodies. *Proc Natl Acad Sci U S A*. 1998; 95(11):6469–73. PMID: [9600990](#)
11. Baba M, Nakajo S, Tu PH, Tomita T, Nakaya K, Lee VM, et al. Aggregation of alpha-synuclein in Lewy bodies of sporadic Parkinson's disease and dementia with Lewy bodies. *Am J Pathol*. 1998; 152(4):879–84. PMID: [9546347](#)
12. Zarranz JJ, Alegre J, Gomez-Esteban JC, Lezcano E, Ros R, Ampuero I, et al. The new mutation, E46K, of alpha-synuclein causes Parkinson and Lewy body dementia. *Ann Neurol*. 2004; 55(2):164–73. Epub 2004/02/03. PMID: [14755719](#)
13. Singleton AB, Farrer M, Johnson J, Singleton A, Hague S, Kachergus J, et al. alpha-Synuclein locus triplication causes Parkinson's disease. *Science*. 2003; 302(5646):841. PMID: [14593171](#)
14. Athanassiadou A, Voutsinas G, Psiouri L, Leroy E, Polymeropoulos MH, Ilias A, et al. Genetic analysis of families with Parkinson disease that carry the Ala53Thr mutation in the gene encoding alpha-synuclein. *Am J Hum Genet*. 1999; 65(2):555–8. PMID: [10417297](#)
15. Lesage S, Anheim M, Letourmel F, Bousset L, Honore A, Rozas N, et al. G51D alpha-synuclein mutation causes a novel parkinsonian-pyramidal syndrome. *Ann Neurol*. 2013; 73(4):459–71. Epub 2013/03/26. doi: [10.1002/ana.23894](#) PMID: [23526723](#)
16. Appel-Cresswell S, Vilarino-Guell C, Encarnacion M, Sherman H, Yu I, Shah B, et al. Alpha-synuclein p.H50Q, a novel pathogenic mutation for Parkinson's disease. *Movement disorders: official journal of the Movement Disorder Society*. 2013; 28(6):811–3. Epub 2013/03/05.
17. Kruger R, Kuhn W, Muller T, Woitalla D, Graeber M, Kosel S, et al. Ala30Pro mutation in the gene encoding alpha-synuclein in Parkinson's disease. *Nat Genet*. 1998; 18(2):106–8. PMID: [9462735](#)
18. Polymeropoulos MH, Lavedan C, Leroy E, Ide SE, Dehejia A, Dutra A, et al. Mutation in the alpha-synuclein gene identified in families with Parkinson's disease. *Science*. 1997; 276(5321):2045–7. PMID: [9197268](#)
19. Li J, Henning Jensen P, Dahlstrom A. Differential localization of alpha-, beta- and gamma-synucleins in the rat CNS. *Neuroscience*. 2002; 113(2):463–78. Epub 2002/07/20. PMID: [12127102](#)
20. Yu S, Li X, Liu G, Han J, Zhang C, Li Y, et al. Extensive nuclear localization of alpha-synuclein in normal rat brain neurons revealed by a novel monoclonal antibody. *Neuroscience*. 2007; 145(2):539–55. Epub 2007/02/06. PMID: [17275196](#)
21. Galvin JE, Schuck TM, Lee VM, Trojanowski JQ. Differential expression and distribution of alpha-, beta-, and gamma-synuclein in the developing human substantia nigra. *Exp Neurol*. 2001; 168(2):347–55. Epub 2001/03/22. PMID: [11259122](#)
22. Zhang L, Zhang C, Zhu Y, Cai Q, Chan P, Ueda K, et al. Semi-quantitative analysis of alpha-synuclein in subcellular pools of rat brain neurons: an immunogold electron microscopic study using a C-terminal specific monoclonal antibody. *Brain Res*. 2008; 1244:40–52. Epub 2008/09/27. doi: [10.1016/j.brainres.2008.08.067](#) PMID: [18817762](#)
23. Huang Z, Xu Z, Wu Y, Zhou Y. Determining nuclear localization of alpha-synuclein in mouse brains. *Neuroscience*. 2011; 199:318–32. Epub 2011/10/29. doi: [10.1016/j.neuroscience.2011.10.016](#) PMID: [22033456](#)
24. Kontopoulos E, Parvin JD, Feany MB. Alpha-synuclein acts in the nucleus to inhibit histone acetylation and promote neurotoxicity. *Hum Mol Genet*. 2006; 15(20):3012–23. Epub 2006/09/09. PMID: [16959795](#)
25. Goers J, Manning-Bog AB, McCormack AL, Millett IS, Doniach S, Di Monte DA, et al. Nuclear localization of alpha-synuclein and its interaction with histones. *Biochemistry*. 2003; 42(28):8465–71. Epub 2003/07/16. PMID: [12859192](#)
26. Oliveira LM, Falomir-Lockhart LJ, Botelho MG, Lin KH, Wales P, Koch JC, et al. Elevated alpha-synuclein caused by SNCA gene triplication impairs neuronal differentiation and maturation in Parkinson's patient-derived induced pluripotent stem cells. *Cell Death Dis*. 2015; 6:e1994. Epub 2015/11/27. doi: [10.1038/cddis.2015.318](#) PMID: [26610207](#)
27. Bendor JT, Logan TP, Edwards RH. The function of alpha-synuclein. *Neuron*. 2013; 79(6):1044–66. Epub 2013/09/21. doi: [10.1016/j.neuron.2013.09.004](#) PMID: [24050397](#)
28. Watson JB, Hatami A, David H, Masliah E, Roberts K, Evans CE, et al. Alterations in corticostriatal synaptic plasticity in mice overexpressing human alpha-synuclein. *Neuroscience*. 2009; 159(2):501–13. Epub 2009/04/14. doi: [10.1016/j.neuroscience.2009.01.021](#) PMID: [19361478](#)

29. Bottner M, Fricke T, Muller M, Barrenschee M, Deuschl G, Schneider SA, et al. Alpha-synuclein is associated with the synaptic vesicle apparatus in the human and rat enteric nervous system. *Brain Res.* 2015; 1614:51–9. Epub 2015/04/22. doi: [10.1016/j.brainres.2015.04.015](https://doi.org/10.1016/j.brainres.2015.04.015) PMID: [25896939](https://pubmed.ncbi.nlm.nih.gov/25896939/)
30. Golovko MY, Barcelo-Coblijn G, Castagnet PI, Austin S, Combs CK, Murphy EJ. The role of alpha-synuclein in brain lipid metabolism: a downstream impact on brain inflammatory response. *Molecular and cellular biochemistry.* 2009; 326(1–2):55–66. Epub 2009/01/01. doi: [10.1007/s11010-008-0008-y](https://doi.org/10.1007/s11010-008-0008-y) PMID: [19116775](https://pubmed.ncbi.nlm.nih.gov/19116775/)
31. Burre J, Sharma M, Tsetsenis T, Buchman V, Etherton MR, Sudhof TC. Alpha-synuclein promotes SNARE-complex assembly in vivo and in vitro. *Science.* 2010; 329(5999):1663–7. Epub 2010/08/28. doi: [10.1126/science.1195227](https://doi.org/10.1126/science.1195227) PMID: [20798282](https://pubmed.ncbi.nlm.nih.gov/20798282/)
32. Hasegawa M, Fujiwara H, Nonaka T, Wakabayashi K, Takahashi H, Lee VM, et al. Phosphorylated alpha-synuclein is ubiquitinated in alpha-synucleinopathy lesions. *J Biol Chem.* 2002; 277(50):49071–6. PMID: [12377775](https://pubmed.ncbi.nlm.nih.gov/12377775/)
33. Duda JE, Giasson BI, Chen Q, Gur TL, Hurtig HI, Stern MB, et al. Widespread nitration of pathological inclusions in neurodegenerative synucleinopathies. *Am J Pathol.* 2000; 157(5):1439–45. PMID: [11073803](https://pubmed.ncbi.nlm.nih.gov/11073803/)
34. Giasson BI, Duda JE, Murray IV, Chen Q, Souza JM, Hurtig HI, et al. Oxidative damage linked to neurodegeneration by selective alpha-synuclein nitration in synucleinopathy lesions. *Science.* 2000; 290(5493):985–9. PMID: [11062131](https://pubmed.ncbi.nlm.nih.gov/11062131/)
35. Fujiwara H, Hasegawa M, Dohmae N, Kawashima A, Masliah E, Goldberg MS, et al. alpha-Synuclein is phosphorylated in synucleinopathy lesions. *Nat Cell Biol.* 2002; 4(2):160–4. Epub 2002/01/29. PMID: [11813001](https://pubmed.ncbi.nlm.nih.gov/11813001/)
36. Queslati A, Fournier M, Lashuel HA. Role of post-translational modifications in modulating the structure, function and toxicity of alpha-synuclein: implications for Parkinson's disease pathogenesis and therapies. *Progress in brain research.* 2010; 183:115–45. Epub 2010/08/11. doi: [10.1016/S0079-6123\(10\)83007-9](https://doi.org/10.1016/S0079-6123(10)83007-9) PMID: [20696318](https://pubmed.ncbi.nlm.nih.gov/20696318/)
37. Anderson JP, Walker DE, Goldstein JM, de Laat R, Banducci K, Caccavello RJ, et al. Phosphorylation of Ser-129 is the dominant pathological modification of alpha-synuclein in familial and sporadic Lewy body disease. *J Biol Chem.* 2006; 281(40):29739–52. Epub 2006/07/19. PMID: [16847063](https://pubmed.ncbi.nlm.nih.gov/16847063/)
38. Tenreiro S, Eckermann K, Outeiro TF. Protein phosphorylation in neurodegeneration: friend or foe? *Frontiers in molecular neuroscience.* 2014; 7:42. Epub 2014/05/27. doi: [10.3389/fnmol.2014.00042](https://doi.org/10.3389/fnmol.2014.00042) PMID: [24860424](https://pubmed.ncbi.nlm.nih.gov/24860424/)
39. Tenreiro S, Reimao-Pinto MM, Antas P, Rino J, Wawrzycka D, Macedo D, et al. Phosphorylation modulates clearance of alpha-synuclein inclusions in a yeast model of Parkinson's disease. *PLoS Genet.* 2014; 10(5):e1004302. Epub 2014/05/09. doi: [10.1371/journal.pgen.1004302](https://doi.org/10.1371/journal.pgen.1004302) PMID: [24810576](https://pubmed.ncbi.nlm.nih.gov/24810576/)
40. Popova B, Kleinknecht A, Braus GH. Posttranslational Modifications and Clearing of alpha-Synuclein Aggregates in Yeast. *Biomolecules.* 2015; 5(2):617–34. doi: [10.3390/biom5020617](https://doi.org/10.3390/biom5020617) PMID: [25915624](https://pubmed.ncbi.nlm.nih.gov/25915624/)
41. Shahpasandzadeh H, Popova B, Kleinknecht A, Fraser PE, Outeiro TF, Braus GH. Interplay between sumoylation and phosphorylation for protection against alpha-synuclein inclusions. *J Biol Chem.* 2014; 289(45):31224–40. Epub 2014/09/19. doi: [10.1074/jbc.M114.559237](https://doi.org/10.1074/jbc.M114.559237) PMID: [25231978](https://pubmed.ncbi.nlm.nih.gov/25231978/)
42. Souza JM, Giasson BI, Chen Q, Lee VM, Ischiropoulos H. Dityrosine cross-linking promotes formation of stable alpha-synuclein polymers. Implication of nitration and oxidative stress in the pathogenesis of neurodegenerative synucleinopathies. *J Biol Chem.* 2000; 275(24):18344–9. Epub 2000/04/05. PMID: [10747881](https://pubmed.ncbi.nlm.nih.gov/10747881/)
43. Jenner P, Olanow CW. Oxidative stress and the pathogenesis of Parkinson's disease. *Neurology.* 1996; 47(6 Suppl 3):S161–70. PMID: [8959985](https://pubmed.ncbi.nlm.nih.gov/8959985/)
44. Yao D, Gu Z, Nakamura T, Shi ZQ, Ma Y, Gaston B, et al. Nitrosative stress linked to sporadic Parkinson's disease: S-nitrosylation of parkin regulates its E3 ubiquitin ligase activity. *Proc Natl Acad Sci U S A.* 2004; 101(29):10810–4. PMID: [15252205](https://pubmed.ncbi.nlm.nih.gov/15252205/)
45. Olanow CW. Oxidation reactions in Parkinson's disease. *Neurology.* 1990; 40(10 Suppl 3):suppl 32–7; discussion 7–9. PMID: [2215972](https://pubmed.ncbi.nlm.nih.gov/2215972/)
46. Gao HM, Kotzbauer PT, Uryu K, Leight S, Trojanowski JQ, Lee VM. Neuroinflammation and oxidation/nitration of alpha-synuclein linked to dopaminergic neurodegeneration. *J Neurosci.* 2008; 28(30):7687–98. Epub 2008/07/25. doi: [10.1523/JNEUROSCI.0143-07.2008](https://doi.org/10.1523/JNEUROSCI.0143-07.2008) PMID: [18650345](https://pubmed.ncbi.nlm.nih.gov/18650345/)
47. Benner EJ, Banerjee R, Reynolds AD, Sherman S, Pisarev VM, Tziperson V, et al. Nitrated alpha-synuclein immunity accelerates degeneration of nigral dopaminergic neurons. *PLoS One.* 2008; 3(1):e1376. doi: [10.1371/journal.pone.0001376](https://doi.org/10.1371/journal.pone.0001376) PMID: [18167537](https://pubmed.ncbi.nlm.nih.gov/18167537/)

48. Prigione A, Piazza F, Brighina L, Begni B, Galbussera A, Difrancesco JC, et al. Alpha-synuclein nitration and autophagy response are induced in peripheral blood cells from patients with Parkinson disease. *Neurosci Lett*. 2010; 477(1):6–10. doi: [10.1016/j.neulet.2010.04.022](https://doi.org/10.1016/j.neulet.2010.04.022) PMID: [20399833](https://pubmed.ncbi.nlm.nih.gov/20399833/)
49. Takahashi T, Yamashita H, Nakamura T, Nagano Y, Nakamura S. Tyrosine 125 of alpha-synuclein plays a critical role for dimerization following nitrative stress. *Brain Res*. 2002; 938(1–2):73–80. Epub 2002/05/29. PMID: [12031537](https://pubmed.ncbi.nlm.nih.gov/12031537/)
50. Paxinou E, Chen Q, Weisse M, Giasson BI, Norris EH, Rueter SM, et al. Induction of alpha-synuclein aggregation by intracellular nitrative insult. *J Neurosci*. 2001; 21(20):8053–61. Epub 2001/10/06. PMID: [11588178](https://pubmed.ncbi.nlm.nih.gov/11588178/)
51. Yamin G, Uversky VN, Fink AL. Nitration inhibits fibrillation of human alpha-synuclein in vitro by formation of soluble oligomers. *FEBS Lett*. 2003; 542(1–3):147–52. PMID: [12729915](https://pubmed.ncbi.nlm.nih.gov/12729915/)
52. Uversky VN, Yamin G, Munishkina LA, Karymov MA, Millett IS, Doniach S, et al. Effects of nitration on the structure and aggregation of alpha-synuclein. *Brain Res Mol Brain Res*. 2005; 134(1):84–102. Epub 2005/03/26. PMID: [15790533](https://pubmed.ncbi.nlm.nih.gov/15790533/)
53. Norris EH, Giasson BI, Ischiropoulos H, Lee VM. Effects of oxidative and nitrative challenges on alpha-synuclein fibrillogenesis involve distinct mechanisms of protein modifications. *J Biol Chem*. 2003; 278(29):27230–40. Epub 2003/07/15. PMID: [12857790](https://pubmed.ncbi.nlm.nih.gov/12857790/)
54. Schildknecht S, Gerding HR, Karreman C, Drescher M, Lashuel HA, Outeiro TF, et al. Oxidative and nitrative alpha-synuclein modifications and proteostatic stress: implications for disease mechanisms and interventions in synucleinopathies. *J Neurochem*. 2013; 125(4):491–511. Epub 2013/03/05. doi: [10.1111/jnc.12226](https://doi.org/10.1111/jnc.12226) PMID: [23452040](https://pubmed.ncbi.nlm.nih.gov/23452040/)
55. Pfeiffer S, Schmidt K, Mayer B. Dityrosine formation outcompetes tyrosine nitration at low steady-state concentrations of peroxynitrite. Implications for tyrosine modification by nitric oxide/superoxide in vivo. *J Biol Chem*. 2000; 275(9):6346–52. Epub 2000/02/29. PMID: [10692434](https://pubmed.ncbi.nlm.nih.gov/10692434/)
56. Hodara R, Norris EH, Giasson BI, Mishizen-Eberz AJ, Lynch DR, Lee VM, et al. Functional consequences of alpha-synuclein tyrosine nitration: diminished binding to lipid vesicles and increased fibril formation. *J Biol Chem*. 2004; 279(46):47746–53. Epub 2004/09/15. PMID: [15364911](https://pubmed.ncbi.nlm.nih.gov/15364911/)
57. Menezes R, Tenreiro S, Macedo D, Santos CN, Outeiro TF. From the baker to the bedside: yeast models of Parkinson's disease. *Microbial cell*. 2015; 2(8):262–79. Epub 27/07/2015.
58. Franssens V, Boelen E, Anandhakumar J, Vanhelmont T, Buttner S, Winderickx J. Yeast unfolds the road map toward alpha-synuclein-induced cell death. *Cell Death Differ*. 2010; 17(5):746–53. doi: [10.1038/cdd.2009.203](https://doi.org/10.1038/cdd.2009.203) PMID: [20019751](https://pubmed.ncbi.nlm.nih.gov/20019751/)
59. Hughes TR. Yeast and drug discovery. *Funct Integr Genomics*. 2002; 2(4–5):199–211. PMID: [12192593](https://pubmed.ncbi.nlm.nih.gov/12192593/)
60. Outeiro TF, Lindquist S. Yeast cells provide insight into alpha-synuclein biology and pathobiology. *Science*. 2003; 302(5651):1772–5. PMID: [14657500](https://pubmed.ncbi.nlm.nih.gov/14657500/)
61. Lazaro DF, Rodrigues EF, Langohr R, Shahpasandzadeh H, Ribeiro T, Guerreiro P, et al. Systematic comparison of the effects of alpha-synuclein mutations on its oligomerization and aggregation. *PLoS Genet*. 2014; 10(11):e1004741. Epub 2014/11/14. doi: [10.1371/journal.pgen.1004741](https://doi.org/10.1371/journal.pgen.1004741) PMID: [25393002](https://pubmed.ncbi.nlm.nih.gov/25393002/)
62. Dixon C, Mathias N, Zweig RM, Davis DA, Gross DS. Alpha-synuclein targets the plasma membrane via the secretory pathway and induces toxicity in yeast. *Genetics*. 2005; 170(1):47–59. PMID: [15744056](https://pubmed.ncbi.nlm.nih.gov/15744056/)
63. Petroi D, Popova B, Taheri-Talesh N, Irmiger S, Shahpasandzadeh H, Zweckstetter M, et al. Aggregate clearance of alpha-synuclein in *Saccharomyces cerevisiae* depends more on autophagosome and vacuole function than on the proteasome. *J Biol Chem*. 2012; 287(33):27567–79. doi: [10.1074/jbc.M112.361865](https://doi.org/10.1074/jbc.M112.361865) PMID: [22722939](https://pubmed.ncbi.nlm.nih.gov/22722939/)
64. Hsu LJ, Sagara Y, Arroyo A, Rockenstein E, Sisk A, Mallory M, et al. alpha-synuclein promotes mitochondrial deficit and oxidative stress. *Am J Pathol*. 2000; 157(2):401–10. Epub 2000/08/10. PMID: [10934145](https://pubmed.ncbi.nlm.nih.gov/10934145/)
65. Su LJ, Auluck PK, Outeiro TF, Yeger-Lotem E, Kritzer JA, Tardiff DF, et al. Compounds from an unbiased chemical screen reverse both ER-to-Golgi trafficking defects and mitochondrial dysfunction in Parkinson's disease models. *Dis Model Mech*. 2010; 3(3–4):194–208. doi: [10.1242/dmm.004267](https://doi.org/10.1242/dmm.004267) PMID: [20038714](https://pubmed.ncbi.nlm.nih.gov/20038714/)
66. Flower TR, Chesnokova LS, Froelich CA, Dixon C, Witt SN. Heat shock prevents alpha-synuclein-induced apoptosis in a yeast model of Parkinson's disease. *J Mol Biol*. 2005; 351(5):1081–100. PMID: [16051265](https://pubmed.ncbi.nlm.nih.gov/16051265/)

67. Junn E, Mouradian MM. Human alpha-synuclein over-expression increases intracellular reactive oxygen species levels and susceptibility to dopamine. *Neurosci Lett*. 2002; 320(3):146–50. PMID: [11852183](#)
68. Parihar MS, Parihar A, Fujita M, Hashimoto M, Ghafourifar P. Alpha-synuclein overexpression and aggregation exacerbates impairment of mitochondrial functions by augmenting oxidative stress in human neuroblastoma cells. *Int J Biochem Cell Biol*. 2009; 41(10):2015–24. Epub 2009/05/23. doi: [10.1016/j.biocel.2009.05.008](#) PMID: [19460457](#)
69. Parihar MS, Parihar A, Fujita M, Hashimoto M, Ghafourifar P. Mitochondrial association of alpha-synuclein causes oxidative stress. *Cell Mol Life Sci*. 2008; 65(7–8):1272–84. doi: [10.1007/s00018-008-7589-1](#) PMID: [18322646](#)
70. Beckman JS. The double-edged role of nitric oxide in brain function and superoxide-mediated injury. *Journal of developmental physiology*. 1991; 15(1):53–9. Epub 1991/01/01. PMID: [1678755](#)
71. Beckman JS, Crow JP. Pathological implications of nitric oxide, superoxide and peroxynitrite formation. *Biochem Soc Trans*. 1993; 21(2):330–4. Epub 1993/05/01. PubMed PMID: [8395426](#)
72. Taus T, Kocher T, Pichler P, Paschke C, Schmidt A, Henrich C, et al. Universal and confident phosphorylation site localization using phosphoRS. *Journal of proteome research*. 2011; 10(12):5354–62. Epub 2011/11/15. doi: [10.1021/pr200611n](#) PMID: [22073976](#)
73. Gotze M, Pettelkau J, Schaks S, Bosse K, Ihling CH, Krauth F, et al. StavroX—a software for analyzing crosslinked products in protein interaction studies. *Journal of the American Society for Mass Spectrometry*. 2012; 23(1):76–87. Epub 2011/11/01. doi: [10.1007/s13361-011-0261-2](#) PMID: [22038510](#)
74. Liu L, Zeng M, Hausladen A, Heitman J, Stamler JS. Protection from nitrosative stress by yeast flavohemoglobin. *Proc Natl Acad Sci U S A*. 2000; 97(9):4672–6. Epub 2000/04/12. PMID: [10758168](#)
75. Dias V, Junn E, Mouradian MM. The role of oxidative stress in Parkinson's disease. *Journal of Parkinson's disease*. 2013; 3(4):461–91. Epub 2013/11/21. doi: [10.3233/JPD-130230](#) PMID: [24252804](#)
76. Danielson SR, Andersen JK. Oxidative and nitrative protein modifications in Parkinson's disease. *Free Radic Biol Med*. 2008; 44(10):1787–94. Epub 2008/04/09. doi: [10.1016/j.freeradbiomed.2008.03.005](#) PMID: [18395015](#)
77. Cassanova N, O'Brien KM, Stahl BT, McClure T, Poyton RO. Yeast flavohemoglobin, a nitric oxide oxidoreductase, is located in both the cytosol and the mitochondrial matrix: effects of respiration, anoxia, and the mitochondrial genome on its intracellular level and distribution. *J Biol Chem*. 2005; 280(9):7645–53. Epub 2004/12/22. PMID: [15611069](#)
78. Nakamura K, Nemani VM, Azarbal F, Skibinski G, Levy JM, Egami K, et al. Direct membrane association drives mitochondrial fission by the Parkinson disease-associated protein alpha-synuclein. *J Biol Chem*. 2011; 286(23):20710–26. Epub 2011/04/15. doi: [10.1074/jbc.M110.213538](#) PMID: [21489994](#)
79. Greenberg DA, Jin K, Khan AA. Neuroglobin: an endogenous neuroprotectant. *Current opinion in pharmacology*. 2008; 8(1):20–4. Epub 2007/10/19. PMID: [17942367](#)
80. Khan AA, Mao XO, Banwait S, Jin K, Greenberg DA. Neuroglobin attenuates beta-amyloid neurotoxicity in vitro and transgenic Alzheimer phenotype in vivo. *Proc Natl Acad Sci U S A*. 2007; 104(48):19114–9. Epub 2007/11/21. PMID: [18025470](#)
81. Watanabe S, Takahashi N, Uchida H, Wakasugi K. Human neuroglobin functions as an oxidative stress-responsive sensor for neuroprotection. *J Biol Chem*. 2012; 287(36):30128–38. Epub 2012/07/13. doi: [10.1074/jbc.M112.373381](#) PMID: [22787149](#)
82. Engelender S, Kaminsky Z, Guo X, Sharp AH, Amaravi RK, Kleiderlein JJ, et al. Synphilin-1 associates with alpha-synuclein and promotes the formation of cytosolic inclusions. *Nat Genet*. 1999; 22(1):110–4. Epub 1999/05/13. PMID: [10319874](#)
83. Kosten J, Binolfi A, Stuver M, Verzini S, Theillet FX, Bekei B, et al. Efficient modification of alpha-synuclein serine 129 by protein kinase CK1 requires phosphorylation of tyrosine 125 as a priming event. *ACS chemical neuroscience*. 2014; 5(12):1203–8. Epub 2014/10/17. doi: [10.1021/cn5002254](#) PMID: [25320964](#)
84. Jones EW. Vacuolar proteases and proteolytic artifacts in *Saccharomyces cerevisiae*. *Methods Enzymol*. 2002; 351:127–50. Epub 2002/06/21. PMID: [12073340](#)
85. Dubiel W, Ferrell K, Pratt G, Rechsteiner M. Subunit 4 of the 26 S protease is a member of a novel eukaryotic ATPase family. *J Biol Chem*. 1992; 267(32):22699–702. Epub 1992/11/15. PMID: [1429620](#)
86. Lee DH, Goldberg AL. Proteasome inhibitors: valuable new tools for cell biologists. *Trends Cell Biol*. 1998; 8(10):397–403. PMID: [9789328](#)
87. Sevcsik E, Trexler AJ, Dunn JM, Rhoades E. Allostery in a disordered protein: oxidative modifications to alpha-synuclein act distally to regulate membrane binding. *J Am Chem Soc*. 2011; 133(18):7152–8. Epub 2011/04/16. doi: [10.1021/ja2009554](#) PMID: [21491910](#)

88. Yu Z, Xu X, Xiang Z, Zhou J, Zhang Z, Hu C, et al. Nitrate alpha-synuclein induces the loss of dopaminergic neurons in the substantia nigra of rats. *PLoS One*. 2010; 5(4):e9956. Epub 2010/04/14. doi: [10.1371/journal.pone.0009956](https://doi.org/10.1371/journal.pone.0009956) PMID: [20386702](https://pubmed.ncbi.nlm.nih.gov/20386702/)
89. Ulrih NP, Barry CH, Fink AL. Impact of Tyr to Ala mutations on alpha-synuclein fibrillation and structural properties. *Biochim Biophys Acta*. 2008; 1782(10):581–5. PubMed doi: [10.1016/j.bbadis.2008.07.004](https://doi.org/10.1016/j.bbadis.2008.07.004) PMID: [18692132](https://pubmed.ncbi.nlm.nih.gov/18692132/)
90. Liu Y, Qiang M, Wei Y, He R. A novel molecular mechanism for nitrated {alpha}-synuclein-induced cell death. *J Mol Cell Biol*. 2011; 3(4):239–49. doi: [10.1093/jmcb/mjr011](https://doi.org/10.1093/jmcb/mjr011) PMID: [21733982](https://pubmed.ncbi.nlm.nih.gov/21733982/)
91. Wang S, Xu B, Liou LC, Ren Q, Huang S, Luo Y, et al. alpha-Synuclein disrupts stress signaling by inhibiting polo-like kinase Cdc5/Plk2. *Proc Natl Acad Sci U S A*. 2012; 109(40):16119–24. Epub 2012/09/19. doi: [10.1073/pnas.1206286109](https://doi.org/10.1073/pnas.1206286109) PMID: [22988096](https://pubmed.ncbi.nlm.nih.gov/22988096/)
92. Nakamura T, Yamashita H, Nagano Y, Takahashi T, Avraham S, Avraham H, et al. Activation of Pyk2/RAFTK induces tyrosine phosphorylation of alpha-synuclein via Src-family kinases. *FEBS Lett*. 2002; 521(1–3):190–4. PMID: [12096713](https://pubmed.ncbi.nlm.nih.gov/12096713/)
93. Ellis CE, Schwartzberg PL, Grider TL, Fink DW, Nussbaum RL. alpha-synuclein is phosphorylated by members of the Src family of protein-tyrosine kinases. *J Biol Chem*. 2001; 276(6):3879–84. PMID: [11078745](https://pubmed.ncbi.nlm.nih.gov/11078745/)
94. Nakamura T, Yamashita H, Takahashi T, Nakamura S. Activated Fyn phosphorylates alpha-synuclein at tyrosine residue 125. *Biochem Biophys Res Commun*. 2001; 280(4):1085–92. PMID: [11162638](https://pubmed.ncbi.nlm.nih.gov/11162638/)
95. Papay R, Zuscik MJ, Ross SA, Yun J, McCune DF, Gonzalez-Cabrera P, et al. Mice expressing the alpha(1B)-adrenergic receptor induces a synucleinopathy with excessive tyrosine nitration but decreased phosphorylation. *J Neurochem*. 2002; 83(3):623–34. Epub 2002/10/23. PMID: [12390524](https://pubmed.ncbi.nlm.nih.gov/12390524/)
96. Chen L, Periquet M, Wang X, Negro A, McLean PJ, Hyman BT, et al. Tyrosine and serine phosphorylation of alpha-synuclein have opposing effects on neurotoxicity and soluble oligomer formation. *J Clin Invest*. 2009; 119(11):3257–65. Epub 2009/10/27. doi: [10.1172/JCI39088](https://doi.org/10.1172/JCI39088) PMID: [19855133](https://pubmed.ncbi.nlm.nih.gov/19855133/)
97. Negro A, Brunati AM, Donella-Deana A, Massimino ML, Pinna LA. Multiple phosphorylation of alpha-synuclein by protein tyrosine kinase Syk prevents eosin-induced aggregation. *FASEB J*. 2002; 16(2):210–2. Epub 2001/12/18. PMID: [11744621](https://pubmed.ncbi.nlm.nih.gov/11744621/)
98. Burai R, Ait-Bouziad N, Chiki A, Lashuel HA. Elucidating the Role of Site-Specific Nitration of alpha-Synuclein in the Pathogenesis of Parkinson's Disease via Protein Semisynthesis and Mutagenesis. *J Am Chem Soc*. 2015; 137(15):5041–52. Epub 2015/03/15. doi: [10.1021/ja5131726](https://doi.org/10.1021/ja5131726) PMID: [25768729](https://pubmed.ncbi.nlm.nih.gov/25768729/)
99. Danielson SR, Held JM, Schilling B, Oo M, Gibson BW, Andersen JK. Preferentially increased nitration of alpha-synuclein at tyrosine-39 in a cellular oxidative model of Parkinson's disease. *Anal Chem*. 2009; 81(18):7823–8. Epub 2009/08/25. doi: [10.1021/ac901176t](https://doi.org/10.1021/ac901176t) PMID: [19697948](https://pubmed.ncbi.nlm.nih.gov/19697948/)
100. Schildknecht S, Pape R, Muller N, Robotta M, Marquardt A, Burkle A, et al. Neuroprotection by minocycline caused by direct and specific scavenging of peroxynitrite. *J Biol Chem*. 2011; 286(7):4991–5002. Epub 2010/11/18. doi: [10.1074/jbc.M110.169565](https://doi.org/10.1074/jbc.M110.169565) PMID: [21081502](https://pubmed.ncbi.nlm.nih.gov/21081502/)
101. Wang X, Liu J, Zhu H, Tejima E, Tsuji K, Murata Y, et al. Effects of neuroglobin overexpression on acute brain injury and long-term outcomes after focal cerebral ischemia. *Stroke; a journal of cerebral circulation*. 2008; 39(6):1869–74. Epub 2008/04/12. doi: [10.1161/STROKEAHA.107.506022](https://doi.org/10.1161/STROKEAHA.107.506022) PMID: [18403737](https://pubmed.ncbi.nlm.nih.gov/18403737/)
102. Chen LM, Xiong YS, Kong FL, Qu M, Wang Q, Chen XQ, et al. Neuroglobin attenuates Alzheimer-like tau hyperphosphorylation by activating Akt signaling. *J Neurochem*. 2012; 120(1):157–64. Epub 2011/04/19. doi: [10.1111/j.1471-4159.2011.07275.x](https://doi.org/10.1111/j.1471-4159.2011.07275.x) PMID: [21496024](https://pubmed.ncbi.nlm.nih.gov/21496024/)
103. Gietz D, St Jean A, Woods RA, Schiestl RH. Improved method for high efficiency transformation of intact yeast cells. *Nucleic Acids Res*. 1992; 20(6):1425. PMID: [1561104](https://pubmed.ncbi.nlm.nih.gov/1561104/)
104. Mumberg D, Muller R, Funk M. Regulatable promoters of *Saccharomyces cerevisiae*: comparison of transcriptional activity and their use for heterologous expression. *Nucleic Acids Res*. 1994; 22(25):5767–8. Epub 1994/12/25. PMID: [7838736](https://pubmed.ncbi.nlm.nih.gov/7838736/)
105. Lee DH, Goldberg AL. Selective inhibitors of the proteasome-dependent and vacuolar pathways of protein degradation in *Saccharomyces cerevisiae*. *J Biol Chem*. 1996; 271(44):27280–4. Epub 1996/11/01. PMID: [8910302](https://pubmed.ncbi.nlm.nih.gov/8910302/)
106. Liu C, Apodaca J, Davis LE, Rao H. Proteasome inhibition in wild-type yeast *Saccharomyces cerevisiae* cells. *BioTechniques*. 2007; 42(2):158, 60, 62. Epub 2007/03/22. PMID: [17373478](https://pubmed.ncbi.nlm.nih.gov/17373478/)
107. Shevchenko A, Wilm M, Vorm O, Mann M. Mass spectrometric sequencing of proteins silver-stained polyacrylamide gels. *Anal Chem*. 1996; 68(5):850–8. Epub 1996/03/01. PMID: [8779443](https://pubmed.ncbi.nlm.nih.gov/8779443/)
108. McLean PJ, Kawamata H, Hyman BT. Alpha-synuclein-enhanced green fluorescent protein fusion proteins form proteasome sensitive inclusions in primary neurons. *Neuroscience*. 2001; 104(3):901–12. Epub 2001/07/07. PMID: [11440819](https://pubmed.ncbi.nlm.nih.gov/11440819/)